CAPITAL UNIVERSITY OF SCIENCE AND TECHNOLOGY, ISLAMABAD

Fabrication of AA7075-ZrB2/B4C Surface Composites using Friction Stir Processing

by

Muhammad Umair Haroon

A thesis submitted in partial fulfillment for the degree of Master of Science

in the

Faculty of Engineering
Department of Mechanical Engineering

2021

This thesis is dedicated to my parents and other family members for their motivation, love and continuous prayers.

CERTIFICATE OF APPROVAL

Fabrication of AA7075-ZrB2/B4C Surface Composites using Friction Stir Processing

by

Muhammad Umair Haroon

(MME193012)

THESIS EXAMINING COMMITTEE

S. No.	Examiner	Name	Organization
(a)	External Examiner	Dr. Syed Hussain Imran Jaffery	NUST, Islamabad
(b)	Internal Examiner	Dr. Waqas Akbar Lughmani	CUST, Islamabad
(c)	Supervisor	Dr. Salman Sagheer Warsi	CUST, Islamabad

Dr. Salman Sagheer Warsi
Thesis Supervisor
December, 2021

Dr. Muhammad Mahabat Khan
Head
Dept. of Mechanical Engineering
December, 2021

Dr. Imtiaz Ahmad Taj
Dean
Faculty of Engineering
December, 2021

Author's Declaration

I, **Muhammad Umair Haroon** hereby state that my MS thesis titled "**Fabrication of AA7075-ZrB2/B4C Surface Composites using Friction Stir Processing**" is my own work and has not been submitted previously by me for taking any degree from Capital University of Science and Technology, Islamabad or anywhere else in the country/abroad.

At any time if my statement is found to be incorrect even after my graduation, the University has the right to withdraw my MS Degree.

(Muhammad Umair Haroon)
Registration No: MME193012

Plagiarism Undertaking

I solemnly declare that research work presented in this thesis titled "**Fabrication of AA7075-ZrB2/B4C Surface Composites using Friction Stir Processing**" is solely my research work with no significant contribution from any other person. Small contribution/help wherever taken has been duly acknowledged and that complete thesis has been written by me.

I understand the zero tolerance policy of the HEC and Capital University of Science and Technology towards plagiarism. Therefore, I as an author of the above titled thesis declare that no portion of my thesis has been plagiarized and any material used as reference is properly referred/cited.

I undertake that if I am found guilty of any formal plagiarism in the above titled thesis even after award of MS Degree, the University reserves the right to withdraw/revoke my MS degree and that HEC and the University have the right to publish my name on the HEC/University website on which names of students are placed who submitted plagiarized work.

(Muhammad Umair Haroon)
Registration No: MME193012

Acknowledgement

First and foremost, I am sincerely thankful to Almighty Allah the most beneficent, ever merciful. Without his gracious consent, nothing is possible.

I would like to express my gratitude to my supervisor Dr. Salman Warsi, who has served as a source of support and guidance for me throughout this project. I am also grateful to my colleagues at IST, because their help, advice and continued support has enabled me to complete this project.

I would also like to express my gratitude to my parents, family, and everyone else who has helped me in any way to achieve this project.

(Muhammad Umair Haroon)

Abstract

Aluminum 7075 alloy has a wide variety of applications in the automotive and aerospace industries; therefore, it is required to enhance its surface properties. Surface integrity can be improved by producing surface composites (SC) and Friction Stir Processing (FSP) is one such technique to produce SC. In this research Friction Stir Processing (FSP) was applied to manufacture a surface composite of aluminum 7075 alloy with Boron Carbide (B4C) and Zirconium Diboride (ZrB2). The preliminary experiment design was carried out using Taguchi L9 orthogonal array with three factors at three levels. Three different tool tilt angles 0, 1 and 2 degrees were used for the experiment. The AA7075 material was reinforced with B4C, ZrB2 and without reinforcement (FSPed). The tool rotational speed was chosen as 450, 710 and 1120 rpm. Using the Taguchi method, the optimum level of each of these parameters was obtained. Wear and hardness testing was performed for the comparison of the results. It was found that ZrB2, 710 rpm and 2-degree tilt angle are the most significant factors for manufacturing of surface composites. Same parameters were chosen to manufacture the ZrB2, B4C and FSPed surfaces. Process was performed on a vertical milling machine for the fabrication of surface composite. Specimen were prepared for the testing of mechanical properties and microstructural characterization from the fabricated composites. Surface hardness, wear resistance and tensile strength were evaluated and microstructure was analyzed. The results showed that when compared to AA7075, the hardness of FSPed, ZrB2, and B4C samples was improved by a factor of 1.20, 1.58, and 1.68, respectively. To determine the Coefficient of friction (COF) for the specimens, a wear test was performed. When compared to base material, the average COF for FSPed, ZrB2, and B4C samples was lowered by 0.645, 0.495, and 0.454. FSPed sample had the highest tensile strength, followed by B4C, ZrB2, and base material (AA7075). Optical microscope, scanning electron microscopy, and energy-dispersive X-ray spectrum were used to examine the microstructure and the composition of the surface composites.

Contents

List of Figures

List of Tables

Abbreviations

AMCs	Aluminum Matrix Composites
B4C	Boron Carbide
COF	Coefficient of friction
EDS	Energy-dispersive X-ray Spectrum
FSP	Friction Stir Processing
FSPed	Friction Stir Processed
FSW	Friction Stir Welding
HAZ	Heat Affected Zone
HV	Hardness Value
MMCs	Matel Matrix Composites
NZ	Nugget Zone
SCs	Surface Composites
SEM	Scanning Electron Microscopy
TMAZ	Thermo Mechanically Affected Zone
UTM	Universal Testing Machine
ZrB2	Zirconium di Boride

Chapter 1

Introduction

1.1 Background

Manufacturing is a vast field of engineering in which different methods are used for the production of goods, equipment, machinery and other useable things. Joining is the one of the branches of manufacturing in which two or more parts are joint together to produce a usable product. The joining of subparts to an assembly can be either permanent or temporary, depending on the requirement. Joining methods are classified into two categories.

- Temporary joining techniques/ Mechanical fastening
- Permanent joining techniques

Temporary joining techniques are needed to link items that will needed to be removed again. Screws, studs, nuts, and bolts are all examples of mechanical fastening. When it comes to permanent joining procedures, these are used to permanently combine pieces when the assembly does not need to be disassembled in the future. Brazing, welding, soldering, and adhesive bonding are all examples of permanent joining. Each joining method has its significance in production and is widely utilized across various industries and applications.

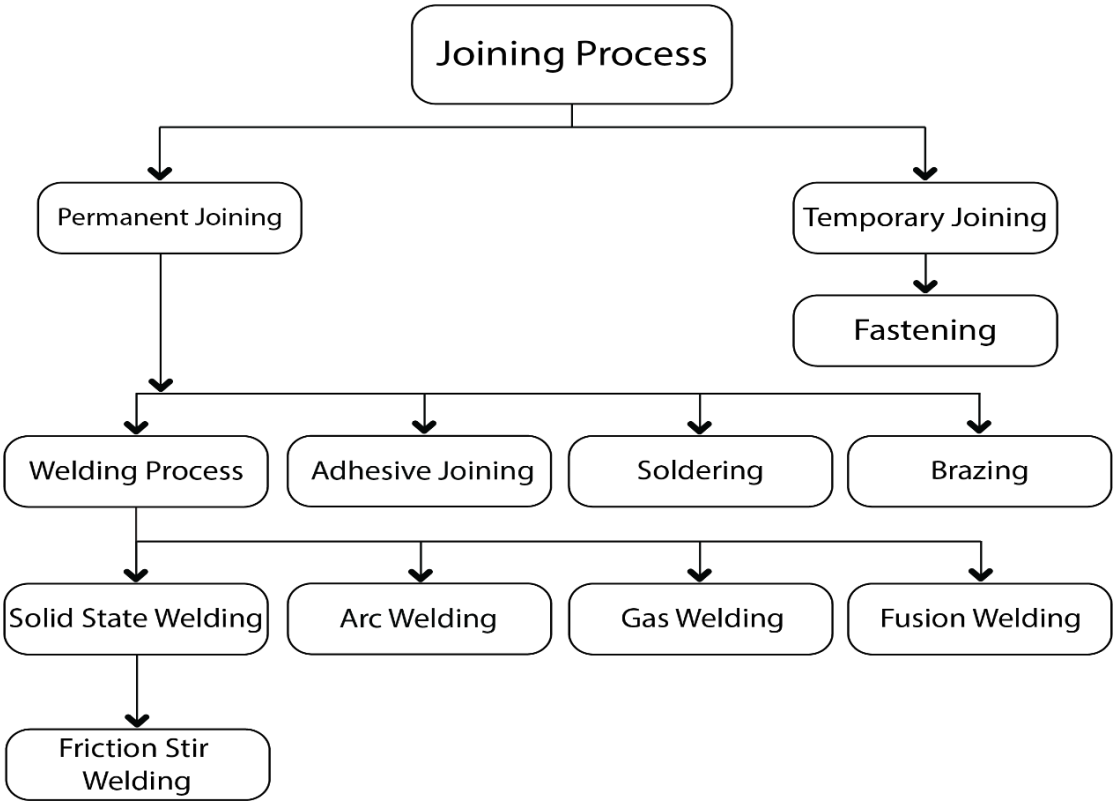

FIGURE 1.1: Classification of the joining processes

Welding is one of the most fundamental techniques used in the industrial sector. Different welding techniques are often used in metal joining, and they are selected based on the requirements, availability, and practicality of the process. Figure 1.1 presents a broad classification of different permanent joining processes used in the industry.

Welding is a manufacturing technique in which components are bonded together by applying heat or pressure to the jointing material. Welding is a popular method of joining metals and thermoplastics together [1].

Different welding processes are used in various applications since a broad categorization of metals and thermoplastics is employed in engineering applications. Some of the principal kinds are shown in the figure above. The fusion-free joining of metals is called solid-state welding. One of important type of solid state welding is friction stir welding (FSW) that is used in many industrial and other daily life applications [2], [3].

Friction stir welding (FSW) is a manufacturing method in which energy is turned into heat at the weldment connection[4]. The FSW process works by bringing atoms of the material joined to equilibrium spacing principally through plastic deformation due to applying pressure at a temperature below the melting point of the base materials, without the addition of filler that melts [5].

An important off-shoot of FSW is Friction Stir Process (FSP) primarily developed for enhancing the material's surface strength. The specimen changes microstructurally as a result of the force produced by the tool. Because of a change in a metal layer, the strength of nearby surfaces also increases. Surface Composites (SC) are created by reinforcing ceramics in powder form (which have a higher strength) over the base material. Reinforcement occurs as the friction between the tool and the metal is a thermomechanical process that produces high temperatures.

Its working principle is that a cylindrical tool with a specially designed tip is rotated and inserted into the targeted area to friction process the desired location within a plate or sheet. The tool's tip is smaller in size and can take on a variety of shapes. The shoulder with a bigger diameter is concentric with the tool's tip. The diameter of the tool-tip and the shoulder length determine the penetration depth; when the rotating tool penetrates the plate's surface, the rotating pin generates friction.

Due to the friction of the revolving pin and base plate, the metal beneath the tip and surrounding regions became softer due to the heating surface. The revolving tool heats the workpiece continuously and plasticizes the metal. The shoulder also regulates the material flow, as material may migrate outward against the tool pin's force. The workpiece and tool are positioned relative to one another during FSP so that the tool traverses the workpiece in overlapping passes until the desired region is treated. The process results in defect-free recrystallized, fine grain microstructure. A stepwise schematic of the FSP process is shown in Fig. 1.2.

FSP has a wide range of applications, some of which are as follows:

1. Fabrication of surface composite

2. Refinement of the microstructure of cast light alloys

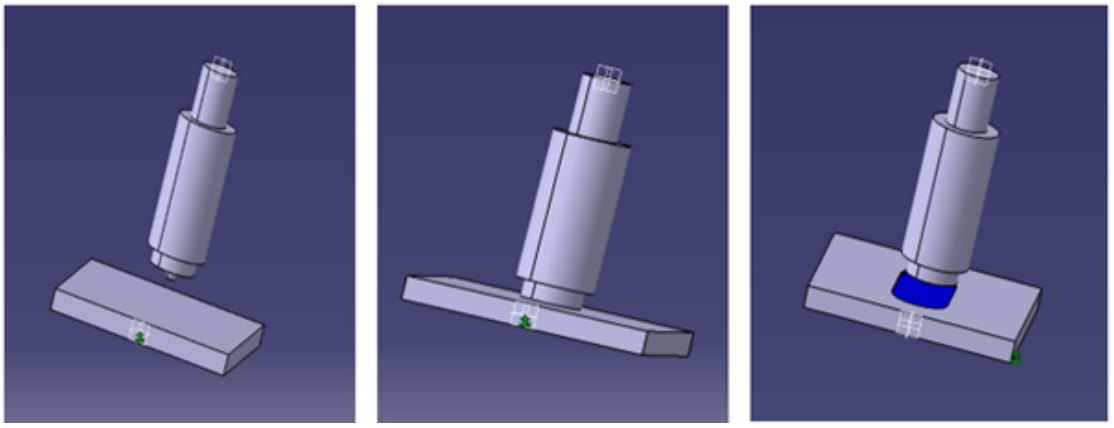

FIGURE 1.2: Stepwise schematic of friction stir processing method

1.2 Research Aim

The aim of this research is to develop a surface composite using friction stir processing for aluminum alloy AA-7075 in order to enhance its mechanical properties.

1.3 Research Objectives

The objectives of the research work are as follows:

1. Identification and selection of suitable parameters for friction stir processing.

2. Manufacture a surface composite by addition of reinforcements (ZrB2 and B4C).

3. Investigate the mechanical properties of manufactures surface composites and compare them with the base metal

4. Comparison of experimental results with the results already published in the literature.

1.4 Research Methodology

1.4.1 Material Selection

Aluminum alloy 7075 (AA7075) is an aluminum alloy based on zinc. AA7075 composition roughly includes 5.6–6.1% zinc, 2.1–2.5% magnesium, 1.2–1.6% copper, and less than a half percent of silicon, iron, manganese, titanium, chromium, and other metals. It possesses superior mechanical properties, is ductile, strong and tough than other aluminum alloys. Due to micro segregation, it is more sensitive to embrittlement than many other aluminum alloys but has significantly better corrosion resistance than the alloys from the 2000 series. It is a widely used aluminum alloy for highly stressed structural applications, extensively used in aircraft structural components. These advantageous properties of Al-7075 alloy make it a valuable material for industrial applications in various industries, including aerospace, marine, and automotive parts. Owing to these properties, Al-7075 has been chosen as a base metal alloy in this research. Furthermore, Al 7075 is a good candidate for development of surface composites (SC) via FSP. Reinforcements such as B4C have been often used by researchers to develop SC [6]–[8]. Such SC have been reported to have better mechanical properties as compared to base metal [9], [10]. In this research, two reinforcements, namely, B4C and ZrB2 have been utilized to fabricate a surface composite with Al 7075. The mechanical properties of the SC have been analyzed and compared.

1.4.2 Experimental Methods

A comprehensive literature review was conducted to extract suitable process parameters for FSP. Setup for the Friction stir processing was designed on a vertical milling machine where the bed of the machine was utilized for the clamping and the milling head was used as a tool holder. Aluminum 7075 was used as a base metal which was subjected to the friction stir processing passes (with and without reinforcements). Reinforcement materials are B4C and ZrB2. Samples were taken

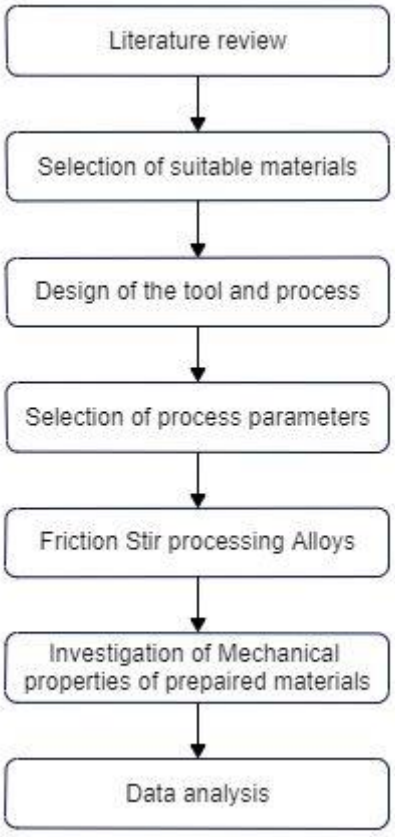

FIGURE 1.3: Research methodology used in this study

from fabricated SC and their mechanical properties were analyzed using Vickers hardness testing machine, pin on disc wear testing machine, Universal Testing machine and Scanning Electron Microscopy.

1.5 Thesis Organization

This thesis is organized into five chapters based on the research work carried out during the course of this MS.

- Chapter 1 presents introduction and the background of this research study. Problem statement, objectives, material selection and experimental methodology are also briefly described in this chapter.
- Chapter 2 presents the literature review on Friction stir welding, Friction stir processing and effect of process parameters.

- Chapter 3 presents the materials, methods and the experimental setup used to carry out this research.
- Chapter 4 presents results and discussion on results in the form of graphical trends that describe the objectives of this research.
- Chapter 5 provides the conclusion and future recommendation on basis of this research study and the research gaps for future studies

Chapter 2

Literature Review

2.1 Welding Process

Welding is a fabrication technique in which two or more parts are fused together by use of heat, pressure, or a combination of the two, resulting in an unbroken joint as the components cool. The most common materials for welding are metals and thermoplastics, however wood can also be welded. A weldment is a term used to describe a fully welded junction [3], [11].

For some materials, special methods and techniques must be used in addition to the material itself. A parent material is a term used to describe the elements that are linked together. Filler or consumable is the term used to describe the material that is used to assist in the formation of the joint [12]. Depending on their shape, these materials may be referred to as parent plate or pipe, filler wire, consumable electrode (for arc welding), and so on. Consumer materials are typically chosen to be close in composition to the parent material, resulting in a homogeneous weld. However, there are situations when a filler with an extremely different composition (e.g., during welding of extremely brittle cast irons).

There are four main types of welding including gas welding, arc welding, resistance welding and solid state welding.

2.2 Friction Stir Welding

Wayne Thomas introduced Friction Stir Welding (FSW) at The Welding Institute (TWI) in 1991[13]–[15]. It is a solid-state joining process that has many advantages over traditional techniques. FSW helps to produce high-strength joints without distortion [16]. It is observed that the operation can weld high-strength aluminum alloys and be used for welding dissimilar metals that are impossible by traditional techniques [5], [17].

FSW is a process in which the high-strength, non-consumable rotating tool is plunged into the joining line of the plates or sheets to be welded [18]. The stirring effect of the tool produces frictional heat and plasticizes the edges of the workpiece and the tool is then translated with the constant feed to create the butt joint [19]. Recently FSW has been used for crack repairing and to remove defects of welding joints, and to improve the mechanical properties of welding joints [3], [20].

The importance of FSW has increased because of its applications in the aeronautical, automotive, and shipping industries. FSW is an energy-efficient and sustainable technique [21], [2]. Friction stir processing is a technique that is based on the principle of friction stir welding. Initially, the process was performed on the FSW joints to enhance the properties of the joint [22]. In recent years FSP gained popularity to fabricate surface composites (SC) of Aluminum, Copper and Magnesium alloy [23], [24].

2.3 Friction Stir Processing

Friction stir processing (FSP) is a process based on the principles of FSW. It was first introduced by Mishra et al. [25]–[27]. Friction Stir Processing (FSP) is a new technique that provides the microstructural change in the surface of metals and controls the near-surface layer of metals. Properties of near surfaces are also modified because of changes in a layer of metals [22], [28]. It is a thermomechanical process that generates high temperatures because of friction between the tool

and the metal. Due to the force applied by the tool, the specimen undergoes microstructural change. The process is used to modify the material's microstructure to enhance its properties [29], [30]. To improve the surface characteristics of metals and alloys, a variety of surface treatment procedures are employed. Among all of those procedures, FSP has the most impact on improving all of those characteristics. The desired objectives for those treatments are increased hardness, improved wear resistance, reflectivity, decoration, and corrosion protection [31].

FSP is also used to develop surface composites with more excellent mechanical properties than its base material. It is a technique that can be used to produce different materials with required properties and can be used at a specific region that need to have high hardness or strength. Surface composites are manufactured by the reinforcement of ceramics materials [8], [23].

FSP can be performed after casting operation to refine the material surfaces. It is used to improve the mechanical properties of cast aluminum alloys [32], [33]. FSP also provides the edge to enhance the properties of specific areas and at required depth [24], [34].

Surface composites are appropriate materials for engineering applications that include surface interactions. Friction stir processing (FSP) is a potential technology for producing surface composites. FSP can improve surface qualities such as abrasion resistance, hardness, strength, ductility, corrosion resistance, fatigue life, and formability without changing the bulk properties of the material [35], [36], [37].

2.4 Process Parameters

The quality of friction stir processing depends upon the process parameters of the process. The basic parameters of friction stir processing are spindle speed (RPM), feed rate (traverse speed) and tilt angle. The properties of the material to be processed and the required properties of the friction stir processed material cause variation in the process parameters. Different studies are conducted on other

parameters such as tool pin profile [38], tool plunge depth [39] and multi passes [40], [41].

Friction stir processing is now commonly used to fabricate surface composites. For the fabrication of surface composite, the amount of reinforcement material depends on the method and size of the reinforcement. Initially, the strategy adopted by the different manufacturers was to produce a single rectangular groove on the surface of the base material and fill the reinforced material into it. However, during the process, reinforced material was displaced forward by the tool, thus resulting in the non-equal distribution of the particles [23]. Therefore, blind holes are preferred to contain reinforced particles at the required place [26]. The size of the groove or blind holes is also the process's parameter, which depends on the percentage of reinforced particles required to manufacture the surface composites.

Challenge is to fabricate the defect-free surface composites, which can only be achieved by optimizing the process parameters [42]. Process parameters are selected to improve the microstructure and the equal distribution of the reinforcement particles to achieve uniform properties throughout the surface [27].

The process parameters of the FSP have been classified in Figure. 2.1. The process parameters must be optimized to achieve the appropriate characteristics of the FSPed materials. The significant parameters include machine variables, reinforcement technique, tool geometry, and the number of passes.

2.5 Machine Variables

The fundamental factors that must be decided prior to the experiment or obtained via trial and error are known as machine variables. Machine variables are constrained by the available setup for a period of time. Machine parameters were kept constant for the process and also have a major effect on FSP so it is important to select optimized machine variables for the process. The optimal mix of factors is chosen to accomplish the quality process, taking into account all resources.

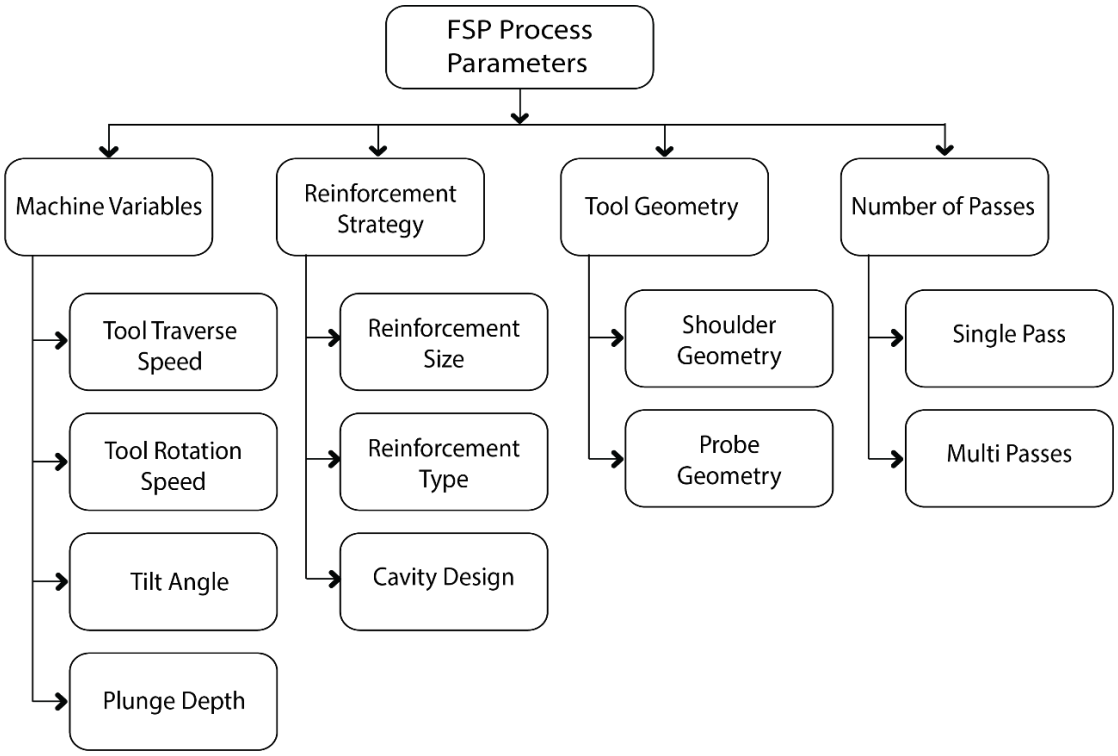

FIGURE 2.1: FSP Process Parameters as presented in [43]

2.5.1 Tool Traverse Speed (mm/minute)

A detailed review of the literature revealed that the mechanical properties of surface composites are affected by FSP process parameters. Higher traverse speed was observed to increase heat input and material flow rates, which facilitated the blending of the filler particles and softened reinforcement materials [43]. Several studies have employed different traverse speeds for FSP. Lower traverse speeds with higher rotation speeds were selected for the better distribution and grain refinement. It has been stated that the tool feed rate is one of the most influential parameters in improving the tensile strength of the manufactured composite [11]. The low feed rate has been generally preferred for the fabrication of various surface composites [44], [36].

2.5.2 Tool Rotation Speed (RPM)

Tool rotation speed refers to the clockwise or anti-clockwise rotation of the tool about its axis. High rotation speeds can provide enough heat to soften the material

whereas low rotation speeds may be causing the less plastic deformation which may lead to unequal distribution [45]. So, for uniform distribution and to avoid particulate clumping, a faster rotational speed is required. High rotational speed, on the other hand, has a negative impact on grain refining due to the high heat input.

According to few studies, the best particle distribution was attained at lower rotation speeds [46]. The rotational speed has an effect on the surface composite produced by FSP. It was observed that the hardness of the generated composite was directly proportional to the tool's rotational speed [36].

2.5.3 Tilt Angle

Tilt angle in FSW/FSP process has been considered as primary parameter. Tilt angle provides extra pressure on the path of the shoulder to enhance the surface finish. Surface finish is a mechanical property that is the essential requirement of the manufacturing processes. Larger tilt angle values increases the heat generation required for the better distribution of the reinforcement and grain structure [47].

Tilt angles normally used in friction stir welding/processing are between 0∘ and 3∘, where zero angles means that tool is perpendicular to the work piece. The tilt angle of the tool was used to contain the material within the path and also to generate required amont of heat [48]. Mechanical properties of the materials fabricated by the FSW/FSP have been found to be dependent on the heat generated and materials flow during the process.

In FSW, the tool tilt angle plays a critical role in weld quality. On the one hand, a non-zero tilt angle ensures contact between the tool shoulder and the work piece; on the other hand, it allows material to flow around the tool more easily. An insufficiently large tilt angle, on the other hand, lifts the pin from the weld root, resulting in defective welds. As a result, selecting the right tool tilt angle is critical. An ideal tool tilt angle ensures that the deformed material is circulated efficiently from the front edge to the back side of the pin by the tool shoulder [49].

2.5.4 Plunge Depth

Plunge depth is another essential factor to consider when trying to improve the microstructure of surface composites. The depth of the plunge is determined by the depth of the reinforcement holes or grooves. It is also determined by the depth of the surface treatment's requirements. The depth of the tool has been found to have a direct impact on the generation of heat. The required contact between the tool shoulder and the base metal is provided by optimizing the tool depth, a significant aspect of friction stir processing for surface treatment [14]. The use of penetration depths that are more than the optimum value may result in the workpiece becoming stuck to the shoulder, the flashing out of particles, the weakening of the processed specimen, as well as the destruction of the specimens themselves. [39].

2.6 Reinforcement Strategy

Before processing, reinforcing particles are introduced over the surface of the matrix material as part of a reinforcement strategy. For the creation of faultless surface composites, a reinforcement strategy is required. According to the study, the reinforcement strategy impacts the mechanical properties of surfaces and their microstructure [30]. Reinforcement strategy have an essential impact on the other parameter selection. Different techniques and methodologies have been adopted by the researchers for the reinforcement. It was discovered that composites made using three gradient grooves reinforcing techniques have higher hardness than previous procedures [43].

2.6.1 Reinforcement Size

Furthermore, the size of the reinforcement particles is a critical consideration in determining the remaining process parameters. Nanoparticles and micro particles can be used as reinforcement in a variety of applications [35]. Following the

selection of the reinforcing size, the size of the groove or drills is determined. Reinforcement particles are critical in the creation of surface composites. The form and size of the reinforcing particle are essential factors to consider in surface composite manufacturing since they influence the surface composite's characteristics. During recrystallization, coarse particles produce bigger grains, while tiny particles decrease grain size.

Composites reinforced with Nano-sized and tougher particles show superior characteristics. The particle size and volume fraction have a significant impact on the characteristics and microstructure of surface composites. It was discovered that Nano-sized reinforced surface composites outperform micro-sized reinforcement. Sudhakar et al. [46] found that the ballistic efficiency of an Al 7075/B4C composite improved owing to the frictional property of the armor surface, which favors damage to the surface of the projectile tip due to the abrasive action of B4C particles on the target. Pol et al. [7] produced various surface composites composed of 25B4C-75TiB2, 50B4C-50TiB2, and 75B4C-25TiB2 reinforced AA7005 surface utilizing friction stir processing and reported that the ballistic efficiency of the 75B4C-25TiB2 surface composite was found to be 1.6 times better than that of the basic alloy.

2.6.2 Reinforcement Type

Reinforcement can be in the form of powder or can be in the form of cylindrical tubes, depending on the application. According to the findings of the researchers, ceramic powders and other metals are used in the production of surface composites and metal matrix composites. [26]. Other than ceramics the industrial wastes are also utilized to manufacture the surface composites by friction stir processing technique to reduce the cost of the material. It is found that the using of industrial wastes as a reinforcement improve the mechanical properties of the base materials. Rice husk ash, pine needle ash, fly ash, sugarcane bagasse ash, coconut shell ash, corn cob ash, and groundnut shell ash have been utilized as reinforcements in the fabrication of cost-effective composites. It has been found that the micro-hardness

of the Al/Rice husk ash surface composite is 40% more than that of aluminum (Matrix material) [50]. Kumar et al. [26] also claimed that fly ash may be used as a reinforcement in the production of copper-based surface composites instead of more expensive ceramic particles.

2.6.3 Cavity Design

By depositing reinforcement on the surface of the base metals during the production process, friction stir processing has been used to create surface composites (SC), Aluminum Matrix Composites (AMC), and other Metal Matrix Composites (MMC). FSP has been employed in a variety of approaches to achieve these goals [43].

- Pasting the reinforcement particles directly on the surface
- Rectangular groove cavity (Single or multi groove pattern)
- Particles in blind holes (single or multi track)
- Particle in blind holes (Zig Zag array)[24]

A rectangular groove and blind holes are commonly adopted for the cavity design [26], [27], [30].

The researchers use a variety of cavity design methods. Groove for the reinforcement was initially common among the researchers. But for the groove type cavity, the particles move along with the tool traverse motion which result in non-equal distribution of the particles. To overcome that a pin less tool was also used by researchers before the FSP pass to avoid the wastage of particles [46], [30]. In the case of blind holes, the center-to-center distance of the holes is critical. If the distance between the holes is larger than it might be possible to have uneven distribution. The center-to-center must be less than the radius of the tools shoulder because half of the leading portion of the tool shoulder was used to control powder

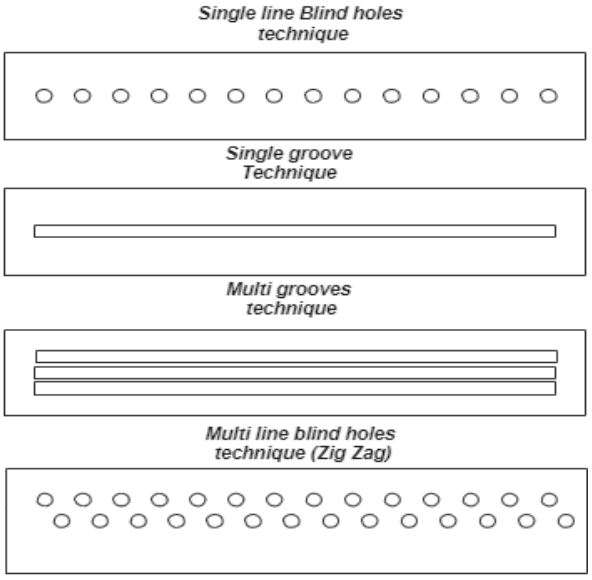

FIGURE 2.2: Types of cavity designs for adding reinforcements

flashing [27]. Single line groove or blind holes produces the region with uneven strength.

2.7 Tool Geometry

Tool geometry is another parameter of FSP/FSW. A tool used for the process is standard of H13 tool steel and surface treated to enhance its strength [2], [10], [16]. Dimensions of the tool can be the parameter, but the essential parts of the tool are its shoulder and the pin.

2.7.1 Shoulder Geometry

The shoulder of the FSP tool provides extra frictional heat due to the large contact surface[48]. Beneath the curvature of the shoulder material is dispersed due to the stirring effect of the pin. The shoulder exerts extra force to provide the surface finish [51]. Bobbin tool geometry was also used in FSW to maintain an equal thickness of the material. It is a double shoulder type tool used to remove the need for tilt angle and plunge force for the process.[52]

2.7.2 Pin Geometry

Tool geometry is one of the essential parameters. Pin profile is part of the tool geometry. Different types of pin profiles are used in FSW. Pin provides the stimulating effect to refine the microstructure and equal distribution of the reinforcement particles[48]. Commonly used pin profiles in FSW/FSP are as below [38]:

1. Straight cylindrical pin (TC)
2. Tapered cylindrical pin (TH)
3. Threaded cylindrical pin (TP)
4. Square pin (SQ)
5. Triangular pin (SC)

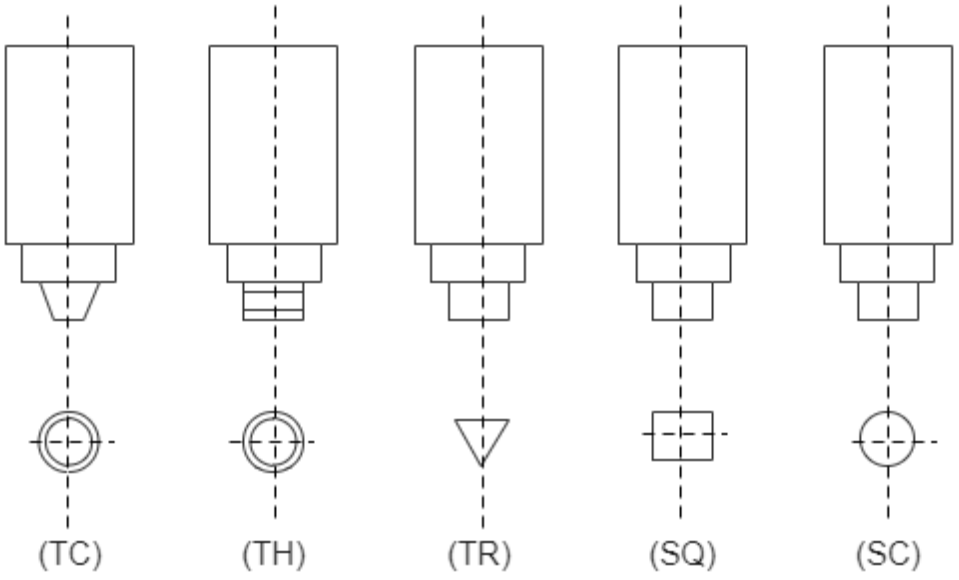

FIGURE 2.3: FSW/ FSP tool pin profiles [38]

Elangovan et al. [38] argued that the square pin profile produces the defect free friction stir processing region when comparing with above mentioned pin profiles at a constant rotational speed. Butola et al. [53] argued that when compared to other characteristics, the tool profile had a substantially less impact on the HV

value. Still, the square tool profile was be the best option among circular and triangular pin profile [16], [38], [53].

2.8 Number of Passes

Several studies have been conducted in recent years to develop surface composites through friction stir processing. Numerous techniques were applied to improve the quality of the processed surface. One of the techniques is single or multi pass friction stir processing. For processing the same area for a single or several times, the term number of passes is employed. The method was designated single pass friction stir processing if it was carried out only once on any path, and multi pass friction stir processing if it was carried out numerous times on the same path [45]. The number of passes is one of the significant parameters considered to improve the material's surface properties [23]. The mechanical qualities of friction stir welding joints were also improved using the multi pass technique. The microstructure of a friction stir welding joint can be enhanced by friction stir processing, resulting in a superior mechanical property joint. Ghangas et al. [54] demonstrated that multiple passes of friction stir welding improves the characteristics of the joint and can be used to treat single pass FSW faults. Similarly friction stir processing has been done in single and multiple passes to achieve the required results. [40]. For different reinforcements, a variable number of passes can be chosen to ensure that the reinforcement particles are distributed evenly.

2.8.1 Process Parameters used in Various FSPed Surface Composites

Process parameters used in different studies to manufacture surface composites are summarized in Table 2.1. The table provides the material's composition, methodology, size of the reinforcement, and machine variables used to manufacture the surface composites.

Table 2.1: Parameters used in various FSPed surface composites

Ref.	BM	Reinforcement	Method and size of reinforcement	Methodology	rpm	Traverse Speed (mm/min)	Tilt angle (deg)
[44]	Al7075	B4C	Groove: Width 1.2mm, Depth 2.5mm, Length 100mm	Different traverse speeds	545	50/78 /120	3
[40]	A359	Si3N4	Groove, Width 2mm, Depth 3mm	One, Two and Three passes	1000	25	0
[8]	Al7075	TiB2/ B4C	Groove: Width 2mm, Depth 3.5mm	Different percentages of TiB2 & B4C	1200	30	3
[30]	Cu	SiC	Groove: Depth 3mm, Width 1.5, 0.5 & 0.3 for one, two & three grooves	Single and multi-groove technique	1000	30	2
[36]	Al5052	ZrO2	holes with a dimension of 1mm diameter & 2mm depth weredrilled	two different rotation speeds and traverse rate	710/ 1400	56/80	0
[55]	AA7075 -T6	B4C	Groove of 160mm length, 2mm width and 1.5mm depth	Comparison of BM FSP with and without B4C	1000	40	2
[56]	Al7075	SiC	Groove width 1.5mm, depth 3mm, length 80mm	Combinations of parameters (RPM, traverse speed & 1&3 passes for each)	1200/ 1400	30/40	3.2
[41]	AA6063	SiC	Groove: 2mm width, 2mm depth	multiple FSP passes(2,4,6,8)	1120	63	2.5
[42]	AA6068	SiC	Groove 2mm width, 2.4mm depth	Single, double & triple pass	1400	40	NA
[23]	Al1060	Cu	Holes 2mm dia, 2mm depth	multiple FSP passes (1,3,5)	1400	60	2
[29]	AA1050	TiO2	Holes 2.5mm dia, 3mm depth	Single and Double pass	1600	20	3
[39]	AA6061	SiC	Groove 2mm depth 2mm width	Varying Tool Plunge depth 0.10 mm to 0.35 mm with difference of 0.5 mm	1400	40	2.5

2.9 Metal Matrix Composites (MMC)

Metal matrix composites are currently widely used in a variety of sectors due to their superior mechanical characteristics. MMC are widely utilized in the transportation, aerospace, and electronics sectors. Friction Stir processing, as previously mentioned, is a method that may be used to make metal matrix composites as well as polymer matrix composites. Rathee et al. [57] compiled data from prior studies and concluded that aluminum was the material of choice for making surface composites. Other than aluminum other metals are also utilized to fabricate surface composites but aluminum is popular among the researchers. Some of the MMC are as under:

- Aluminum Metal Matrix Composites
- Magnesium Metal Matrix Composites
- Copper Metal matrix Composites
- Titanium Metal Matrix Composites
- Steel Metal Matrix Composites
- Metal Matrix Composites using shape memory alloy as reinforcement

2.10 Polymer Matrix Composites

Nowadays, polymer matrix composites are also extensively utilized. Polymers with high surface strength are used in coating and tribology applications. Metals, polymers, and ceramics are added to polymeric matrix composites according on the requirements. Two factors are mainly responsible for the characteristics of mature PMC. The first variables to examine are the type, distribution, and volume percent of reinforcement. The second factor to examine is composite manufacturing method. There are many techniques for fabricating PMC in use today. The use

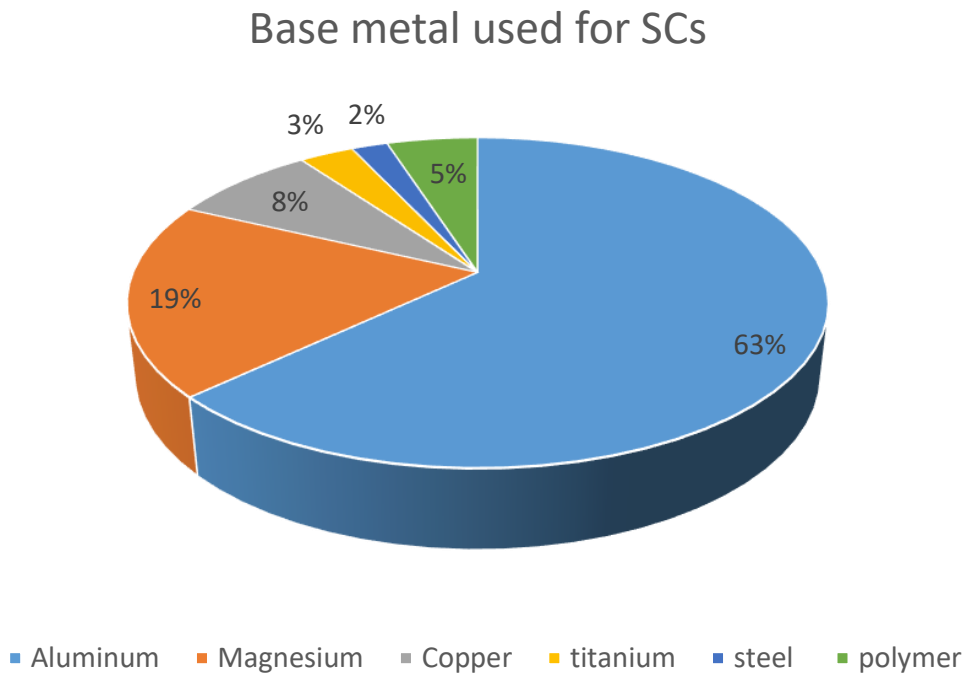

FIGURE 2.4: Base material used to manufacture SCs by FSP [57]

of metallic and ceramic particles as reinforcements in PMCs has been a focus of study for the last 20 years. FSP is used in the manufacturing of PMCs in addition to MMC. In contrast to MMC, however, there is less literature available for fabricating PMCs through FSP.

2.11 Properties Affected by Friction Stir Processing

Friction stir processing is a manufacturing technique that has been used to improve the properties of materials, particularly their surface properties. When FSP is applied to any material, the surface undergoes various changes as a result of the force applied, the tool's stirring, and the heat generated by friction. The microstructure of the materials is affected by the aforementioned changes. The change in microstructure improves the materials' mechanical, tribological, fracture, and corrosion properties [45]. The properties affected by the FSP process are depicted in Figure 2.5.

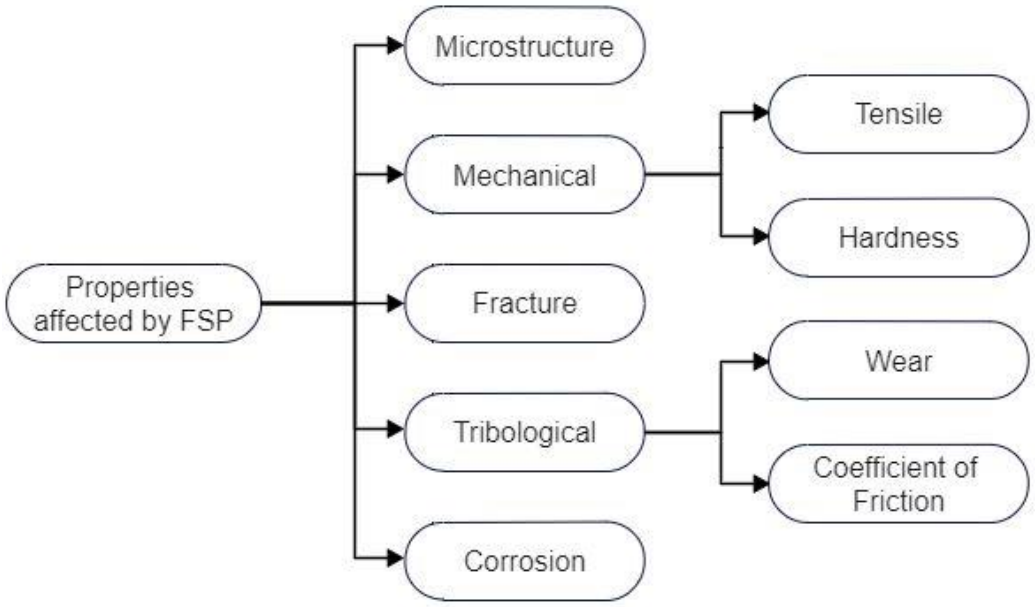

FIGURE 2.5: Properties affected by FSP as presented in [45]

2.12 Microstructural Properties

During FSW/FSP, the combination of severe plastic deformation and high-temperature exposure causes microstructural and composition development within the stirred zone, as well as precipitate dissolution and particle size reduction within and around the stirred zone. Three separate zones, stirred (nugget) zone, thermo-mechanically affected zone (TMAZ), and heat-affected zone (HAZ), have been observed based on microstructural characterization of grains and precipitates. The effects of microstructural changes in various zones on post-weld mechanical characteristics are important. As a result, a number of researchers have looked into the microstructural changes during FSW/FSP [58]. Jain et al. [29] studied the effect of titanium dioxide on microstructure after single and double pass friction stir processing. Zones of FSW/FSP are illustrated in figure below. At an optimum speed of 1000 rpm and a feed rate of 30 mm/min, friction stir processing of copper with various volume percentages of BN was effectively carried out by Thankachan [59]. The grain size is decreased and the particles are evenly distributed in the copper solution, according to microstructural analysis.

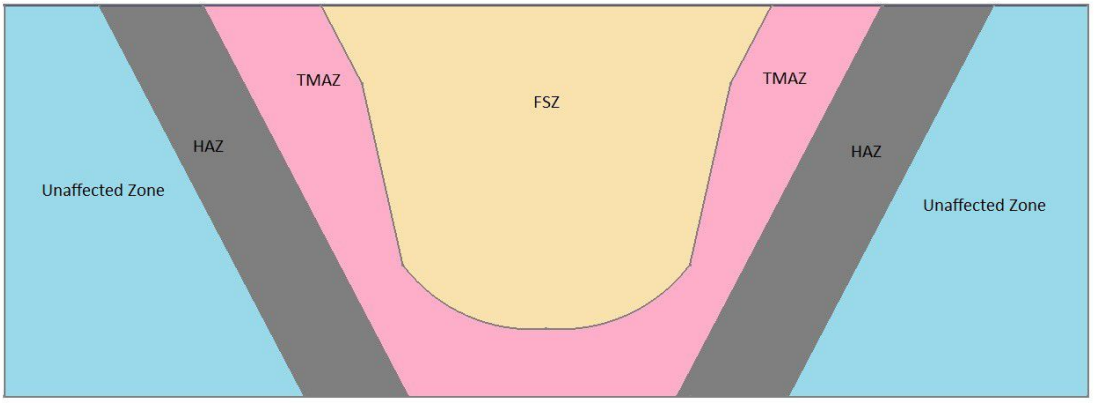

FIGURE 2.6: FSW/FSP microstructural zones

2.12.1 Friction Stir Zone/Nugget Zone (NZ)

As a result of the intense plastic deformation and frictional heating that occurs during the FSW/FSP, a recrystallized fine-grained microstructure is formed within the stirred zone. This region is referred to as the nugget zone (or weld nugget). In the nugget zone, under certain FSW/FSP conditions, an onion ring structure was observed to exist [34]. The dislocation density in the interior of recrystallized grains is typically low, especially in the early stages of recrystallization. The nugget zone contains a high density of sub-boundaries, sub grains, and dislocations, according to certain researchers who have studied the microscopic recrystallized grains of the nugget zone [58]. Various geometries of nugget zone have been observed depending on processing parameters, tool geometry, workpiece temperature, and heat conductivity of the material. Essentially, there are two main types of nugget zones: basin-shaped nuggets that widen near the upper surface and elliptical nuggets [8], [34].

2.12.2 Thermo-Mechanically Affected Zone (TMAZ)

Friction stir welding/processing produces a fine grain structure while also generating heat due to the tool's stirring effect. Because of the high spin and friction, the adjacent region of the nugget zone is influenced by the heat produced and the mechanical deformation [60]. The combination of temperature and deformation

creates a zone with characteristics distinct from both the nugget zone and the base metal. This transition phase is known as thermo-mechanically affected zone. The TMAZ underwent plastic deformation, however due to insufficient deformation strain, recrystallization did not occur in this zone [51][61]. However, due to high-temperature exposure during FSW/FSP, certain precipitates disintegrated in the TMAZ. Of course, the degree of dissolution is determined by TMAZ's thermal cycle. In addition, it was discovered that the grains in the TMAZ have a high density of sub-boundaries [60].

2.12.3 Heat Affected Zone (HAZ)

As thermo-mechanically affected zone undergoes high temperature and plastic deformation. Heat transfers beyond the TMAZ and effect the near region that known as heat affected zone (HAZ). This zone is affected by the thermal cycle and does not experience any plastic deformation. As heat affected zone undergoes only the temperature rise that's why the grain structure remains same as base material [13]. The weakest section of the FSW weld joint is at HAZ, according to Azeez et al. [2] they also reported that if the FSW joint is efficient, the sample should fracture at the HAZ when subjected to tensile force.

2.13 Mechanical and Tribological Properties

Many studies have been published in recent years to investigate the various qualities that are improved or affected by FSP. The majority of that is focused on mechanical and tribological properties, and because the augmentation of mechanical and tribological properties is attributable to a change in microstructure of the material, the researchers also looked into the characterization of the grain structure. The basic mechanical property of the materials that was affected by FSP is surface hardness and tensile strength. Wear qualities, on the other hand, have drawn the attention of researchers. Bharti et al. [62] investigated the influence

of FSP on the Al-6000 series, as well as the hardness qualities. Butola et al. [53] investigated the micro-hardness and microstructural properties of fabricated Al-7075 surface composites to optimize FSP process parameters using Taguchi technique. Prabhu et al. [42] studied the effect of multi pass friction stir processing on mechanical and tribological properties of AA6068/SiC surface composites. An increase in micro-hardness and tensile strength up to 2.5 and 1.25 times and the decrease of 1.5 times wear rate compared to base material was reported in this study. Similarly, when the hardness, tensile, and wear properties of the new material are compared to those of the base material, a considerable improvement is seen.

Mouli et al. [47] optimized the process parameters to obtain the better hardness of AA7075/SiC surface composites and suggested that a tool rotational speed of 1125 rpm, a tool traverse speed of 50 mm/min, and a tool tilt angle of 30 should be used to manufacture AA7075/SiC surface composite. Pol et al. [7] manufactured the AA7005 surface composites with varied weight fractions of TiB2 and B4C and compared to base material, the hardness of the surface composites increased by 70 percent. Patel et al. [1] examined the micro-hardness of dissimilar FSW joint (Aluminum to polymer) fabricated at different tool rotation and traverse speeds. Huang et al. [23] manufactured the Al-Cu surface composites with 1,3 and 5 passes and revealed that micro hardness was increased with increase in number of passes. Patel et al. [1] evaluated the tensile strength of dissimilar material. Where the highest tensile strength of the composite was obtained at rotational speed of 500 rpm and traverse rate 40 mm/min. Saina et al. [63] investigated the tensile, hardness and wear properties of aluminum matrix composites by addition of MoS2 and Zn. When compared to Zn base composite, the wear rate of the MoS2 base composite was increased, while the hardness of the Zn base composite was higher than that of the MoS2 base composite. The wear rate and hardness of both composites were found to be higher when compared to the basic material. Sharma et al. [6] created a hybrid surface composite by combining B4C and MoS2 and found that the hybrid surface composite (75 percent B4C+25 percent MoS2) had better wear resistance than mono surface (B4C) composite while having a

lower hardness. The hybrid surface composite with equal amount of B4C and MoS2 had the lowest wear resistance among the surface composites, which may be ascribed to the higher proportion of soft MoS2 and lower hardness. Periasamy et al. [37] investigated the impact of AA7075 surface composites of SiC and Gr produced by FSP on friction and wear. Because of the reinforcement, the hardness of manufactured surface hybrid Al 7075/SiC & Gr composites increased from 85Hv to 90Hv. Because of the lubricating characteristic of Gr in Al 7075, the wear rate was decreased. Table 2.3 lists the tests carried out in the various studies listed in Table 2.1.

2.14 Fracture and Corrosion Properties

Friction stir welding and processing are techniques that include the penetration of a spinning tool into the surface. As a consequence, heat was produced, and grains were displaced or distorted plastically. Stresses were generated as a result of the heat and stirring of the tool, and surfaces may fracture. This fracture is caused by the material's characteristics, cavity development, and grain structure [40]. Fracture of the materials fabricated by FSW/FSP was studied with the help of Scanning electron Microscopy and optical microscopes. The behavior of the fracture can be studied after tensile testing of the materials. Kumar et al. [30] manufactured the surface composites by single and multi-groove techniques and applied tensile testing on the specimens and studied the nature of fracture with SEM. The results of fractography revealed that ductility was reduced on both surface composites when compared to base material. Akbari et al. [15] applied friction stir lap welding of aluminum and copper and studied the lap shear fracture loading of several FSW conditions. Corrosion, on the other hand, is the response of the environment on the substance, which results in dissolution and changes the characteristics of the material. Corrosion is the worst thing that has to be minimized, and it is a material's adversary. Many methods are being developed by researchers to minimize the impact of corrosion. Friction stir processing is another method used to minimize the effects of corrosion [31]. Kumar et al. [64] have

shown that raising the NaCl concentration improved the corrosion resistance of AA7075 regardless of the quantity of TiC. Kumar et al. [26] reported the improved corrosion resistance of the composite over pure copper is due to homogeneous particle dispersion in the matrix, grain refinement of the manufactured composite, and the lack of voids or pores. Bharti et al. [36] produced Al5052/ZrO2 surface composites by using FSP. Aluminum 5052 is widely used in the military, marine, and aerospace sectors. This alloy proved to be an ideal alloy for marine ships and other applications due to its corrosion-resistant characteristics and high tensile strength. However, owing to its poor hardness and wear resistance characteristics, its maritime uses are restricted. As a result, a method to enhance its hardness and wear resistance is required. This alloy's characteristics may be enhanced by including a composite on its surface. ZrO2 has improved wear resistance, high strength, high hardness, good chemical resistance, and high fracture toughness. As a result, it may be a viable choice for reinforcement. Kumar et al. [65] used FSP to assess corrosion resistance and mechanical characteristics of stir casted AA7075/SiC micro and nanocomposites. And it was observed that casted composites had extremely poor mechanical strength, but after using FSP, the tensile strength was increased by 190 percent and the elongation was increased by 854 percent. SEM was also used to investigate the mechanism of failure of as cast and FSPed surfaces following tensile testing.

2.15 AA7075 Surface Composites

After understanding FSP, the primary objective here is to investigate the effect of process parameters on the development of AA7075 surface composites. The detailed purposes of previous research on Al-7075 alloy provide insight into the design and behavior of composite materials processed under various operating conditions. An overview of recent research has been compiled on aluminum 7075 surface composites, with the type of reinforcement employed and the results obtained by the study being listed in the Table 2.2.

Table 2.2: Overview of recent research on AA7075 Surface composites

S. No. Ref.	Base Material	Reinforcement	Results
1. [44]	Al7075	B4C	The hardness of the surface composite increased by a factor of 1.3 to 1.6 to base metal.
2. [8]	Al7075	TiB2/B4C	The hardness of all the SC is higher and the wear rates are lesser than the base metal.
3. [56]	Al7075	SiC	Hardness increased with traverse and rotational speeds and increased 1.65-2.15 times compared to the base material. Wear properties were also improved.
4. [66]	Al7075	TiN	Wear and friction performance are higher (34 to 56% & 1.7 to 23%). Hardness compared to parent metal increases (10 %) and ductility is found to be lower (22 to 50%)
5. [67]	Al7075	SiC	Enhancement in both strength and ductility. Improvement in the hardness levels with increasing SiC content.
6. [50]	Al7075	Rice Husk Ash	The Microhardness increased for all SCs. The tensile properties of all SCs were lower than the parent AA7075-T6 alloy. Zigzag pattern SCs gave higher tensile strength than the linear pattern and groove pattern.
7. [64]	Al7075	TiC	The hardness was found to be increasing on increasing the volume fraction of TiC. The corrosion rate of all the samples got increased
8. [68]	Al7075	Coconut Shell	Unprocessed parent material Al7075 has higher mechanical properties than the processed and fabricated Al7075/CCSA sample. Surface integrity was greatly improved.
9. [69]	Al7075	SiC-BN	Improved the wear rate and increased the hardness due to SiC particles and BN increased the machinability.
10. [70]	Al7075	SiC/Gr	Microhardness, wear rate and coefficient of friction increased significantly
11. [71]	Al7075	B4C	Microhardness of the FSPed and FSPed+ B4C sample was 25% & 50%-100% higher than the base metal. Wear resistance also increased with an increase in the hardness of the specimens.

TABLE 2.3: Tests performed to investigate effects of FSP

Base Material	**Reinforcement**	**Testing**
AA7075	B4C	Micro hardness using Vickers hardness test at a load of 300gm and dwell 10 sec. Wear test has been carried out for eachsample at load of 60N
A359	Si3N4	The tensile test was conducted for all three kinds of samples having a single pass, two passes and three passes along with unprocessed A359
AA7075	TiB2/B4C	Micro Hardness testing of the samples at equal distance from the stir zone center line. Wear rate of AA7075 and the FSPed samples
Cu	SiC	Tensile Testing, micro hardness testing and wear test
Al5052	ZrO2	Microhardness and wear behavior
AA7075-T6	B4C	Tensile Testing and micro hardness testing
AA7075	SiC	Dry- sliding wear behavior and micro hardness
AA6063	SiC	Micro Hardness of fabricated composites
AA6068	SiC	Hardness test, Friction and wear behavior
Al1060	Cu	microhardness and wear behavior
AA1050	TiO2	microhardness and sliding wear behavior
AA6061	SiC	Effect of tool plunge depth on distribution of SiC particles

Chapter 3

Experimental Methodology

The methodology describes the entire procedure that was followed in order to complete the project. The procedure adopted for preparation of the workpiece and FSP is discussed in detail in this chapter.

3.1 Tool-Workpiece

A schematic diagram of the workpiece and how the FSW tool will approach the workpiece is depicted in Fig. 3.1. Different views of the process are to elaborate the complete process. All dimensions are in mm and the tilt angle is shown in degree. The isometric view of the process is shown in Fig. 3.2. FSP is a non-cutting process on a milling machine and requires a heavy-duty tool that may undergo very high stress during the process. During the operation, the tool rotates at high rpm, lower feed, and the tool's shoulder contain all the material in that region. Due to the friction of the tool's shoulder, a high amount of heat was also generated. This process is also complete without coolant. That's why the tool of the FSP should be of hard material. For this purpose, H13 and D2 tool steels materials are available and can be used for FSP.

The following sections provide an explanation of the specific procedures that were followed to complete this project.

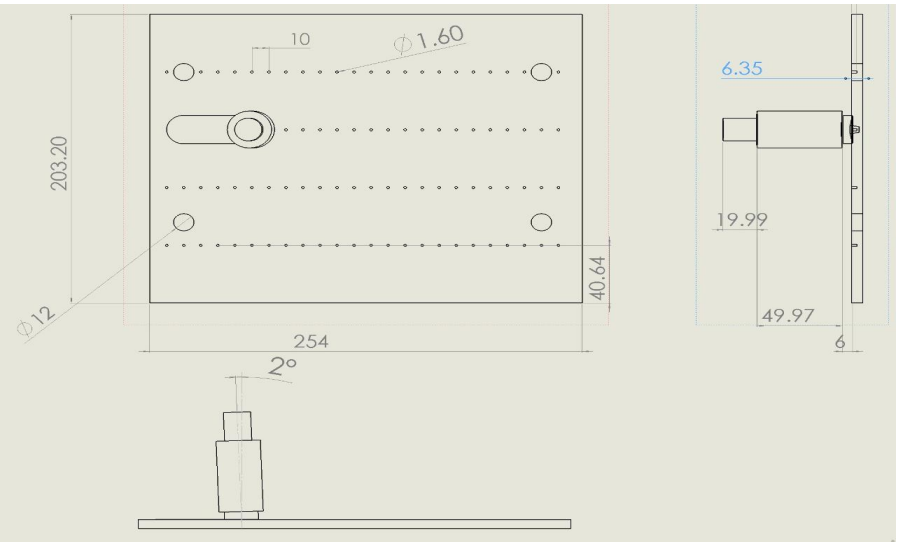

FIGURE 3.1: Schematic Diagram of the process

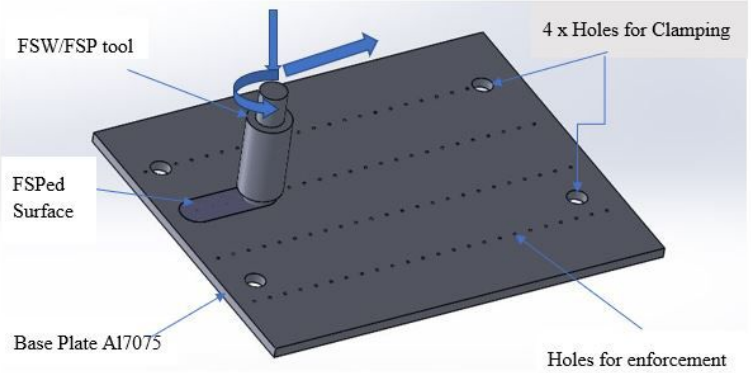

FIGURE 3.2: Isometric views of the process

3.2 Cutting of Aluminum Plate

The plate of Aluminum 7075 is used for the project. Two plates of aluminum 7075 were cut of equal dimensions. One is used as a specimen and the other is as a base plate. The base plate is clamped right under the specimen to control the heat produced during the process. Dimensions of the plates are as under:

TABLE 3.1: Dimensions of the Base plate (AA7075)

Dimensions of the base plate (A17075)	
Length	254 mm
Width	203.20 mm
Thickness	6.35 mm

FIGURE 3.3: Layout on an Aluminum plate and marking

3.3 Layout of the Workpiece

Following layout was done on the workpiece plates.

1. Marking the position of the holes for clamping the aluminum plate on the milling bed according to the T-slots.
2. Dividing the plate into five equal spaces and mark the straight lines that are the tool's path.
3. On every tool path, mark the points having a center-to-center distance of 10 mm.
4. Center punching is further done on the marked points.

The layout of the plate is shown in figure 3.3.

3.4 Development of Setup

3.4.1 FSW Tool

D2 Tool Steel is a flexible, high-carbon, high-chromium, air-hardening tool steel characterized by a relatively high achievable hardness and a microstructure that

FIGURE 3.4: D2 material bar for the FSP tool

contains several large, chromium-rich alloy carbides. D2 Tool Steel is available in a variety of sizes and shapes. Compared to other metals and abrasive materials, these carbides exhibit excellent wear resistance when in sliding contact with them. Other steels with improved toughness or wear resistance are available. Still, the combination of wear resistance and toughness, as well as tool performance, pricing, and a wide variety of product forms, makes D2 an excellent choice.

3.4.2 Designing of Tool

It is required to manufacture the tool according to the requirements. By using AutoCAD, the design of the tool was finalized and the dimensions were set. Especially the design of the tip and the shoulder of the tool. Detail diagram of the Friction stir processing tool was illustrated in figure. 3.9 for the understanding. All the dimensions are in mm.

3.4.3 Machining of Tool

The FSP tool is also of the circular cross-section, manufactured on the lathe machine. The tool was manufactured according to the design parameters. Several lathe processes were involved in completing the manufacturing of the tool. As the material of the FSP tool was very hard so the lathe tool used for machining the

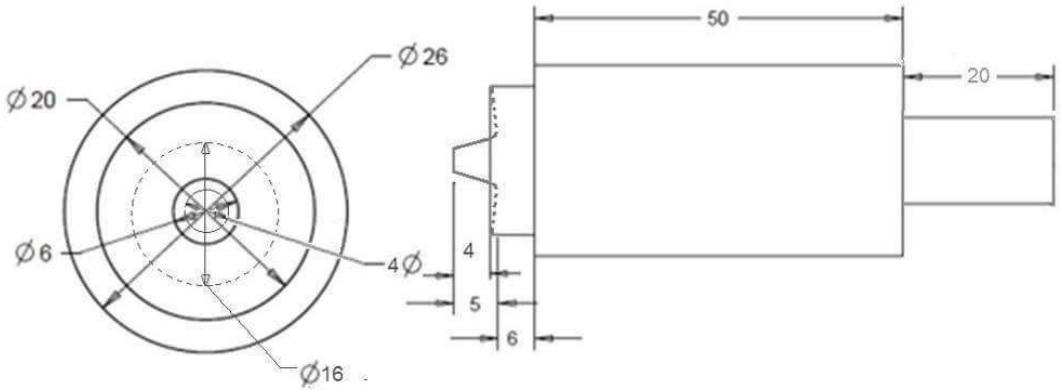

FIGURE 3.5: Drawing of FSP tool (Front and Side View)

FIGURE 3.6: FSP Tool

D2 material was the carbide tip tool. For the machining of the hard materials, the rpm of the lathe was kept low to meet the cutting speed of the material. Tool shoulder and pin required a smooth surface for better finishing that's the reason to kept constant feed while lathe process. The angle of the tool-tip and the angle on the shoulder are the measurements that are technically very important to achieve. These two angles play a very vital role in FSP.

3.4.4 Clamping of the Tool

Collet chuck is used to clamp the milling cutters on a vertical milling machine. Collet chuck is different in size and specific collets are used for the particular

diameter tools. The diameter of the FSP tool is designed according to the size of the collet available because it's also essential to clamp the tool very rigidly.

The non-cutting profile of the FSP tool is the reason for providing the high frictional force required for the procedure. The high rotational speed of the tool, along with the frictional force, makes it absolutely necessary to double-check the clamping of the tool. After the FSP pass, it is also extremely crucial to tighten the tool because the tool was subjected to significant vibrations throughout the operation and may have become loosened.

3.5 Drilling Stopper

It is attached with the vertical scale of the drilling machine for increasing the accuracy of drilling depth. A depth of 3 mm is mandatory for equal filling of the powder. Drilling stopper provides the ease to create the number of blind holes of the same depth.

3.6 Drilling

Following drills were carried out on the plates:

1. Holes of 12mm for the clamping of the base plate.
2. Drilling of 12mm also on the specimen for the clamping.
3. Drilling of 1.6mm and depth of 3mm on the path of the tool as marked in layout, which is at the distance of 10mm.
4. Finishing of the holes of 1.6 mm is then done for clearing the cavity for the reinforcement. The holes can be finished with the reaming tool, which is not available quickly so that it can be done with a smaller pin of about 1.5 mm diameter.

3.7 Clamping

Clamping the plate is also a critical task during FSP because, On the Milling machine, the tool rotates at very high rpm and at automatic feed, which is 16 mm/minutes. For that purpose, four bolts of M-12 have been used on the Aluminum plates at the corners according to the slots of the milling bed. M12 bolt is shown in Fig. 3.7.

FIGURE 3.7: M12 bolt for the clamping

T-slots provide the space for the head of bolts for clamping. But when the nuts of the bolts are tightened, the head of the bolts also rotates and can't find the grip required, so the rod of 6 mm diameter was welded with the head of the bolts to get extra grip as shown in Fig. 3.8.

FIGURE 3.8: M12 bolt after welding with rod

T-bolts can also be used for this purpose, but from the market survey, the available T-bolts are large in diameter, so it was decided to use the above technique and

weld the rods with the heads of each bolt to get the required grip. Four bolts for clamping are shown in Fig. 3.9.

FIGURE 3.9: Clamping kit for the Aluminum plate

3.8 Clamping and Alignment of Specimen

As discussed, the base plate is right under the specimen, so the base plate was attached to the milling bed before clamping the specimen. The specimen was clamped to the base plate as previously explained because the holes on both plates are aligned. Bolt nuts were tightened with a torque wrench and ensured that the holes for the enforcement on the specimen are also aligned with the milling machine's Y-axis, which ran parallel to the milling bed's slots.

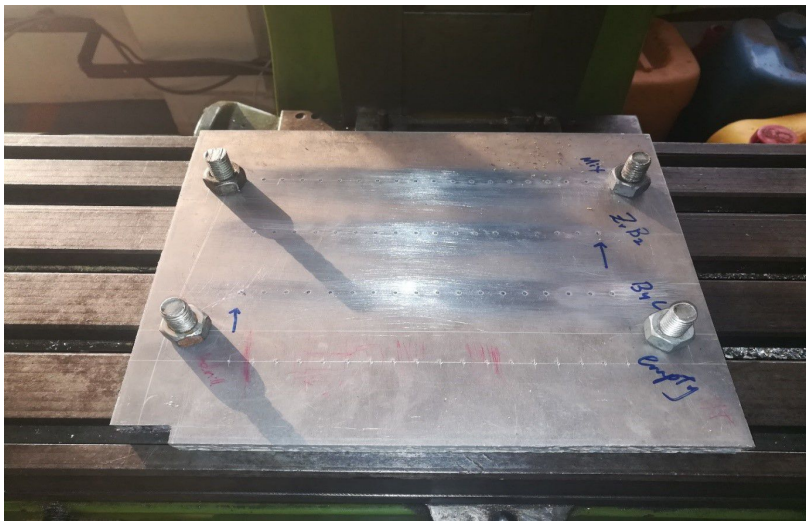

FIGURE 3.10: Clamping of AA7075 plate for FSP on Milling Bed

3.9 Design of Experiment (DoE)

Base on literature review, tilt angle, type of reinforcement and rotational speed have been identified as the key factors for the manufacturing of surface composites using fiction stir processing technique. Different levels of these factors have been studied and applied by the past researchers to manufacture surface composites. However, it is not economically viable to perform friction stir processing on all the parameters previously applied to manufacture the surface composites of AA7075. So, it was decided to select best levels of above-mentioned factors by using Taguchi's Design of Experiments (DOE).

Following are the factor levels selected for experiments. DOE is an experimental method in which the effect of process parameters can analyzed by varying them instantaneously at different levels. Based on literature, three factors (type of reinforcement, rotation speed and tool tilt angle) at three-levels have been selected as shown in Table 3.2.

Table 3.2: Factors and their levels for DOE

Sr. No.	Factor	Levels
1	Tilt Angle (degree)	0, 1, 2
2	Reinforcements	B4C, ZrB2, FSPed
3	Rotational speed (rpm)	450, 710, 1120

Taguchi's L9 orthogonal array was used for the design of experiments. The complete experimental plan was developed with the help of MINITAB (version 17) software as shown in Table 3.3.

Friction stir processing was performed on the above mentioned nine combinations of the process parameters selected by using Taguchi's L9 Orthogonal array. Where the D2 conical pin profile tool was used at the constant traverse speed of 16

mm/min for all the FSP passes. Reinforcements were added by creating the 1.6 mm diameter blind holes on the surface of the AA7075 aluminum plate at center-to-center distance of 10 mm and constant depth of 3 mm.

Friction stir processing was performed on vertical milling machine. Hardness and wear testing was performed on the processed surfaces for the evaluation of the results. Hardness testing was carried on micro vicker hardness tester and wear testing was performed on MICRO TEST Tribometer system. The results were compared and the optimum level of each parameter was obtained. Main Effects plot shows the effectiveness of the process parameters on the results.

Using the FSP surfaces the HV and COF values for each specimen is calculated. MINITAB (version 17) software is used to perform analysis of this Taguchi experiment design. The main effects plot for means indicates the variation of response variables (HV and COF values) with process parameters i.e., type of reinforcement, rotation speed and tool tilt angle. The horizontal dashed line represents the mean value of the response variable.

Table 3.3: Taguchi's L9 Orthogonal Array

Sr. No.	**Reinforcement**	**RPM**	**Tilt Angle**
1	B4C	450	0
2	B4C	710	1
3	B4C	1120	2
4	ZrB2	450	1
5	ZrB2	710	2
6	ZrB2	1120	0
7	FSPed	450	2
8	FSPed	710	0
9	FSPed	1120	1

Figure 3.11 indicates that the maximum hardness value was achieved by adding ZrB2 as reinforcement. And also by increasing rotational speed to 710 rpm and 2°tilt angle.

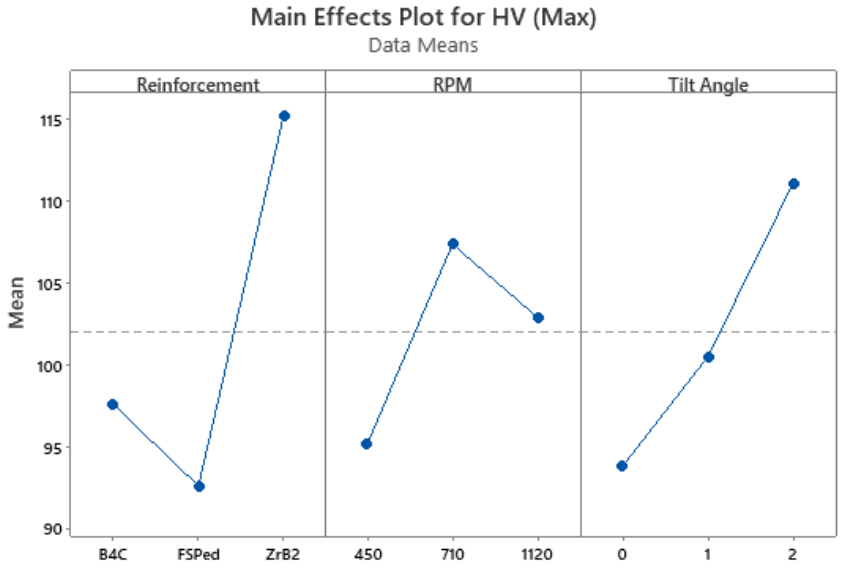

FIGURE 3.11: Main effects plot for HV (Max)

Figure 3.12 shows the main effects plot for COF value. The best values of COF were same in term of type of reinforcement and the 2°tilt angle. But the best value of COF in term of rotational speed was achieved at 1120 rpm.

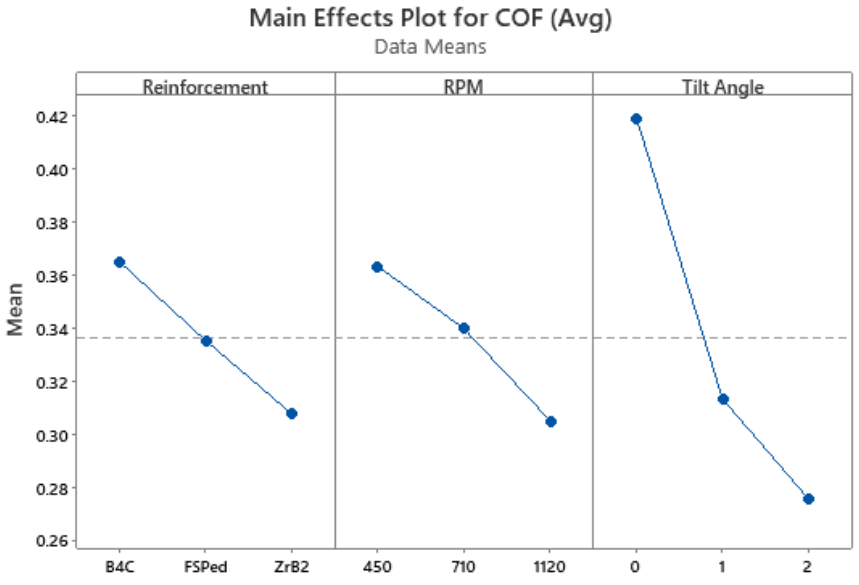

FIGURE 3.12: Main Effects plot for COF(Avg)

Error bar chart for maximum HV is shown below:

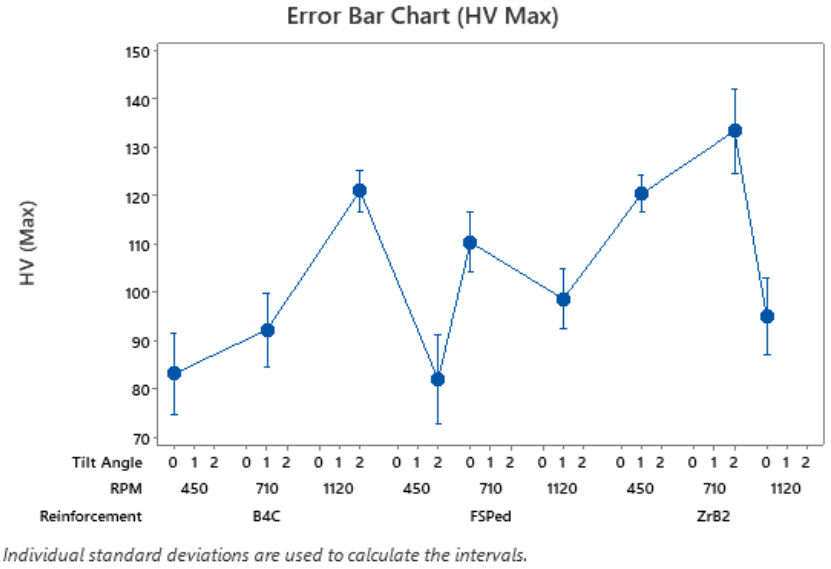

FIGURE 3.13: Error Bar Chart of HV (Max)

Error bar chart for the average COF is shown below.

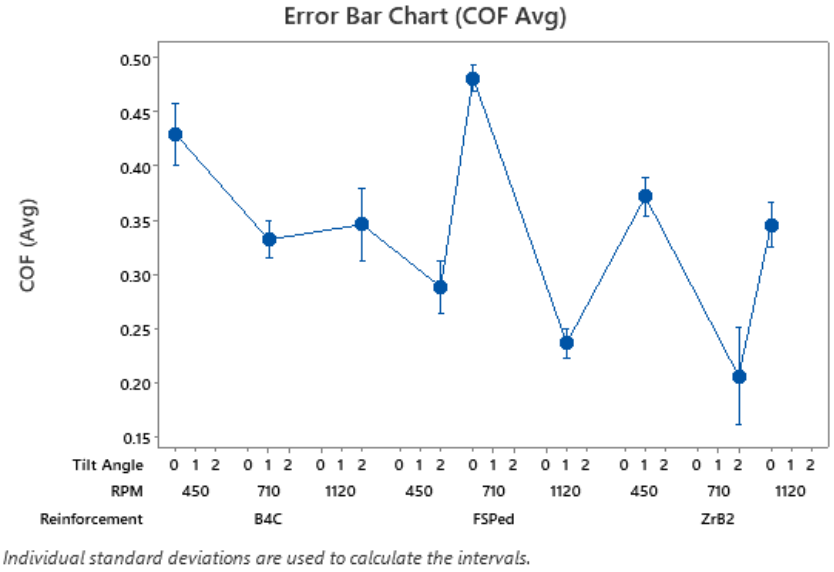

FIGURE 3.14: Error Bar chart of COF (Avg)

3.10 Selection of Process Parameters

After performing the design of experiment the optimum parameters were applied to manufacture the FSPed, ZrB2 and B4C surfaces for further testing and comparison

of the results with the base material. 710 and 1120 rpm are ideal for Friction Stir Processing based on Taguchi experiment performed for the manufacturing of surface composites. It has been decided to select 710 rpm based on the conditions of the working environment. FSP can also conducted at 1120 rpm; however, milling machine produce vibrations by the high rotational speed. It also noted that the percentage error between selection of 710 and 1120 rpm is less than 8% from main effects plot for COF. So, it was decided to perform FSP at 710 rpm instead of 1120 rpm. The parameters selected for the process are as under:

Table 3.4: Parameter specified for FSP

Serial no.	**Process parameters**	**Preferred-Value**
1	Rotational speed	710 rpm
2	Traverse speed	16 mm/min
3	Tilt angle	2 degrees
4	Number of passes	Single-pass
5	Pin Type	Conical, cylindrical pin
6	Shoulder Diameter	20 mm

3.11 Processes of FSP

The following are the steps involved in friction stir processing:

3.11.1 Drilling

The first process is drilling, in which the tool-tip penetrates in the plate. The drilling process continued until the depth was completed and the shoulder of the tool touched the surface. Friction stir welding/processing tool tip is not same like drilling bit or milling cutter. The pin doesn't have cutting edges so it was necessary to penetrate the tool at a low traverse speed. It is also preferred to penetrate the tip in steps and the dwell time between the steps can be selected according to the properties of the base metal.

3.11.2 Generation of Heat

Next process of the friction stir process is the heat generation. It was also discussed in previous chapter that the generation of the heat is a critical step of the process. The stirring effect of the tool pin and the friction of the shoulder generate the heat in the stirring zone. Generation of the heat due to the pin and the shoulder increase the temperature of the base material which cause the temperature difference in the near region of stirring zone.

3.11.3 Heat Transfer

The heat transfer and plasticization of the material at the tool pin and under the shoulder of the tool is caused by an increase in temperature. It was at this point that the tool was rotating at a high rpm but without moving in any direction. It is necessary to dwell for a period of time in order to generate the heat required for the procedure.

3.11.4 Tool Progression

Tool progression is the term used to describe the linear movement of the tool. The motion of the tool along the path at a constant traverse speed is a tool progression. More heat is generated by the combined action of tool rotation and traverse speed, which may lead to refining of the plasticized grains. The tool swept the material into the pass with its shoulder, and it also exerted force to keep the material in the pass.

3.11.5 Material Accumulation

As the tool advances, materials accumulate, and auto traverse feed ensures that the powder is spread uniformly along the tool's path as the agency moves forward. As

a result of the forces exerted by the agency, metal is plasticized and its mechanical characteristics are improved.

3.11.6 Dispersion

Dispersion is the process of transferring the metal from one spot to another. In FSP, the material disperses as the tool rotates and due to the tilt angle, the localized force is applied to increase its mechanical properties.

3.12 Friction Stir Processing Passes

Three passes are processed of friction stir processing for the experiment. Theses passes are explained briefly as follows:

3.12.1 FSPed Pass

The FSPed pass is the pass that does not have any reinforcements applied. It should be noted that there is no powder in the path of the tool. The purpose of the empty pass is to investigate the material's properties after being subjected to FSP. The tool's force and the heat factor contribute to improving the material's strength and other mechanical properties.

3.12.2 AL+ B4C Pass

The pass in which the path of the tool is drilled at a distance of 10mm is designated as Al+ B4C. The drill has a diameter of 1.6mm and a depth of 3mm, respectively. The B4C powder was then injected into the cavities, and the process was completed by using friction stir processing. As B4C is a hard material, it is required to increase the dwell time before tool progression for the required temperature to be achieved.

3.12.3 AL+ ZrB2 Pass

The Al+ ZrB2 pass is analogous to the Al+ B4C pass in that the cavities are filled with ZrB2. As with B4C in the previous path, the holes were adequately filled and the process was completed using FSP.

3.13 Preparation of Specimens for Mechanical Testing and Microstructure Inspection

After friction stir processing, specimens for hardness, tensile, wear, and metallography was prepared. Several machines are used to prepare the samples according to the requirement of the testing setup. CNC wire cut and hack saw were used for cutting the specimen of the FSPed aluminum plate. Different sizes of the specimens are required for further testing of Base metal and each FSPed portion/pass. A cross-sectional view was needed for the hardness testing and the metallography and top surfaces were required for wear testing, whereas three tensile testing specimens were also cut out from each pass.

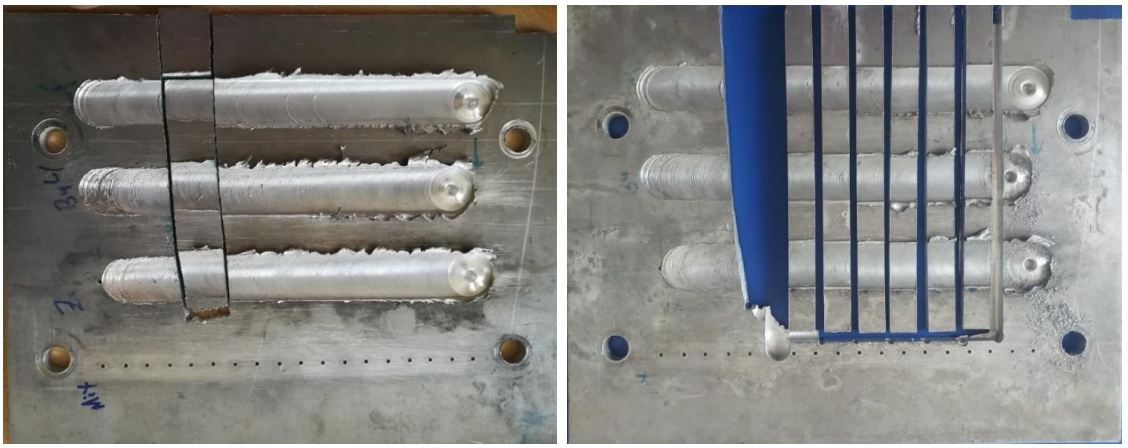

FIGURE 3.15: Cutting of plate for preparation of specimens

Because a hacksaw is required to produce parallel/rectangular surfaces, smooth file was used to remove burs, mount the peace on the milling, and create a parallel and smooth specimen surface. Also, cut it further to produce one sample of each

Table 3.5: Sample Identification (ID) as per testing

Serial No.	**Samples Identification**	**Tensile Testing**	**Wear Testing**	**Hardness Testing**	**Metallography**
1	Al7075	T1A, T1B, T1C	W1	H1	M1
2	FSPed	T2A, T2B, T2C	W2	H2	M2
3	ZrB2	T3A, T3B, T3C	W3	H3	M3
4	B4C	T4A, T4B, T4C	W4	H4	M4

Table 3.6: Dimension of the tensile test specimens

The dimensions of tensile test specimens	
Total Length	60 mm
Gauge Length	20 mm
Width of sample	12 mm
Thickness	6 mm
Width of reduced section	8 mm

pass for wear, metallography, hardness, and tensile testing, as well as three for tensile testing.

3.13.1 Samples Identification (ID)

For identification, each sample is assigned a unique identification code. Four sets of samples are prepared for the comparative study for the tests as mentioned above. Because the pieces are the same size and there is a chance that they will be mixed up during testing, they must be marked for identification. So, each sample was designated a code which is mentioned below in the table.

3.13.2 Tensile Testing Specimens

Tensile testing specimens are cut out perpendicularly from each pass to conduct the tests. The FSPed sections have a 20 mm width as a result, 20 mm gauge length samples that were symmetric were prepared from each pass for comparison. It was also suggested that at least three pieces from each part and the base metal be prepared to validate the results. The dimensions of the specimens are mentioned in the table, and the samples are shown in the Figure below.

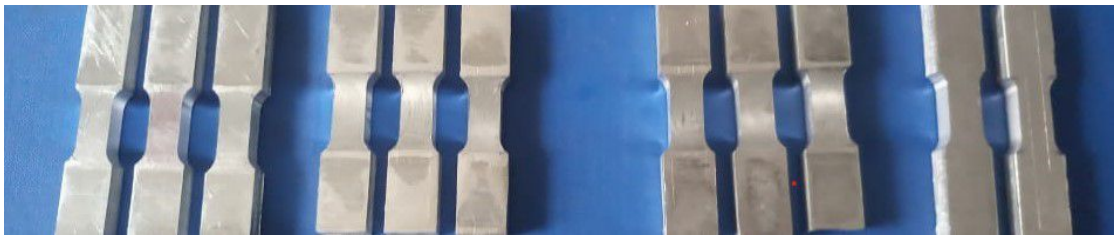

FIGURE 3.16: Specimens for tensile testing

FIGURE 3.17: Wear testing specimens

3.13.3 Wear Testing Specimens

Specimens for the wear testing were prepared from all four surfaces and then subjected to the testing. Rectangular samples of 20 X 12 mm were cut out from each path for the testing.

3.13.4 Hardness Specimen

Hardness profiles for four different regions must be calculated and compared to one another to complete the task. For this to be possible, the cross-sectional areas must be polished and have a parallel surface for the indentation. For the hardness testing, it was essential to remove the parallel strips from the plate to prepare four specimens for the test. The specimens are 20 X 20 mm in size.

3.13.5 Specimens for Metallography

Aside from that, specimens for metallography are also prepared from this plate. Metallography is the study of the physical structure of metals, and it is a branch of science. A cross-sectional view was required to conduct metallography, which is

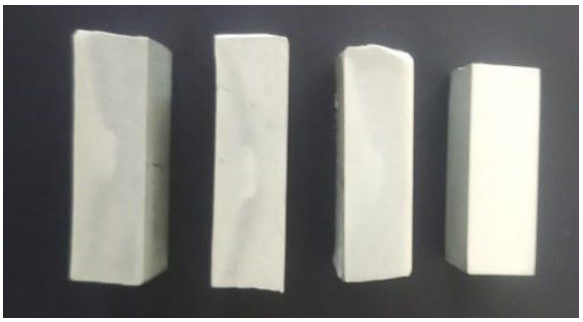

FIGURE 3.18: Specimens for hardness testing

FIGURE 3.19: Specimen's for metallography

why parallel samples were cut from the plate, which was then polished and etched in preparation for further investigation. The specimens are 20 X 12 mm in size.

3.13.6 Grinding and Polishing of Samples

The material's hardness can be calculated using a micro-Vickers hardness testing machine, which requires flat surfaces. The specimen is then ground and polished using a polishing machine. It is also necessary for metallography. All of the samples of hardness and metallography are ground with sandpapers of various grades. The grinding procedure is depicted in Fig. 3.20

FIGURE 3.20: Grinding and polishing of the specimens

3.13.7 Etching

The samples were chemically etched for a better view of the microstructure. Keller's reagent was used to etch the samples. The etched time was 8 to 15 seconds and then washed with warm water. Compositions used for etchant are in Table.3.6.

TABLE 3.7: Keller's Reagent Composition

Constituent	**Distilled Water**	**Nitric Acid**	**Hydrofluoric Acid**	**Hydrochloric Acid**
Concentration (mL)	90	5	2	3

The etched surface shows the contrast of the FSP zone and the near-surface zone, which was further examined in metallography and other microstructural studies. But by the human vision, it is also clear that the affected zone is slightly different from the other surface.

Chapter 4

Results and Discussions

Mechanical testing of the specimens was carried out after the preparation of the specimens. In this section, the processed portion of the Aluminum plate was inspected to find out the enhancement in mechanical properties of Aluminum 7075. A hardness, tensile and wear test was performed to determine the mechanical properties of the treated surface and compare the samples. A metallography test was carried out to examine the microstructure of the base metal and the surfaces that were treated.

4.1 Hardness Testing

In most cases, the Vickers hardness test technique (also known as the micro-hardness test method) is employed when working with tiny components, thin sections, or case depths. Based on an optical measurement device, the Vickers technique is used to measure distances. The Microhardness test technique, ASTME-384, provides a light load range. An indentation is made with a diamond indenter, measured and translated to a hardness value by a computer. It is quite beneficial when evaluating a wide range of materials; nevertheless, the test sample must be well polished to estimate imprints' size accurately. A Vicker hardness testing machine was used to calculate the hardness of the plate (Specimen). The

hardness testing results are according to the Micro-Vicker hardness testing machine. Micro Vicker hardness tester calculates the value of axis according to the microstructure view of indenter and the force applied by the indenter. The values are shown below. The hardness profile also shows the variation of hardness in the FSPed region. During the test, the following factors are assumed to be constant.

- Test load applied is HV0.2 (1.961 N)
- Duration Time is 5 seconds

The mean hardness values of the specimen before and after the FSP and reinforcing were compared. The study's goal was to achieve variability in outcomes, which it did. The hardness results are presented in the graph below. Surface composites have a higher hardness than the FSPed sample, and the FSPed sample has a higher hardness than the parent metal sample (Al7075). The highest hardness of the material was discovered in the stirring zone, with values dropping as one moved away. The hardest surface composite was Al7075+ B4C, which had the maximum hardness rating. The graph below shows the hardness profiles of base metal and FSPed specimens. The parent metal (Al7075) was found to have an average hardness of 86.82HV. In the FSPed, ZrB2, and B4C passes, the hardness was increased significantly. In a stirred zone, the highest hardness found in the FSPed pass was HV105.

The hardness of the surface was raised as a result of the localized force and the recrystallization of the surface structure. The addition of ZrB2 particles raised the surface hardness over that of the FSPed pass, resulting in a micro-Vickers hardness value of HV113 to HV137. The higher hardness value is due to the grain refining and recrystallization of the particles provided by ZrB2. The addition of the B4C particle boosted the base metal's hardness as well. Because B4C is the hardest ceramics material, its hardness value is higher than that of the ZrB2 pass. The hardness ratings are listed as HV122 through HV146. Rana et al. [44] also presented similar values of HV for Al7075/B4C surface composite at traverse speed and rotational speed of 50 mm/min and 545 rpm and also observed that

the hardness was reduced with an increase in traverse speed. Karpasand et al. [8] studied the effect of amount of B4C and TiB2 particles and presented the same trend of HV values of (Al7075+100 % B4C).

The values of the maximum hardness of all the specimens are shown below.

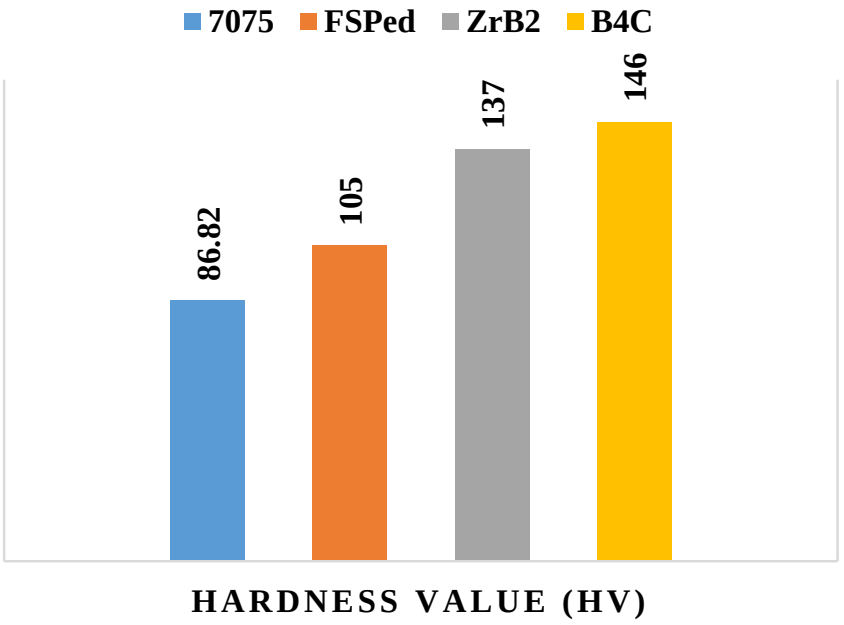

FIGURE 4.1: Maximum hardness value (HV) of the specimens

From the base material (Al7075), the FSPed, ZrB2, and B4C passes have improved by a factor of 1.20, 1.58, and 1.68 respectively. It can be noticed that the average hardness of the FSPed plate without reinforcement is slightly higher than that of the base plate. Reactions involve microstructural changes during FSP as a result of heat production and strong plastic deformation. The development of dynamic recrystallization causes grain change into fine and equiaxed form, which increases hardness[6], [26].

The hardness profile of FSPed (with and without reinforcement) and the base metal was presented below in graph. The cross-sectional profile from the center of the specimens were plotted which indicates the highest value of hardness in the nugget zone. Manufacturing the surface composites with an equal distribution

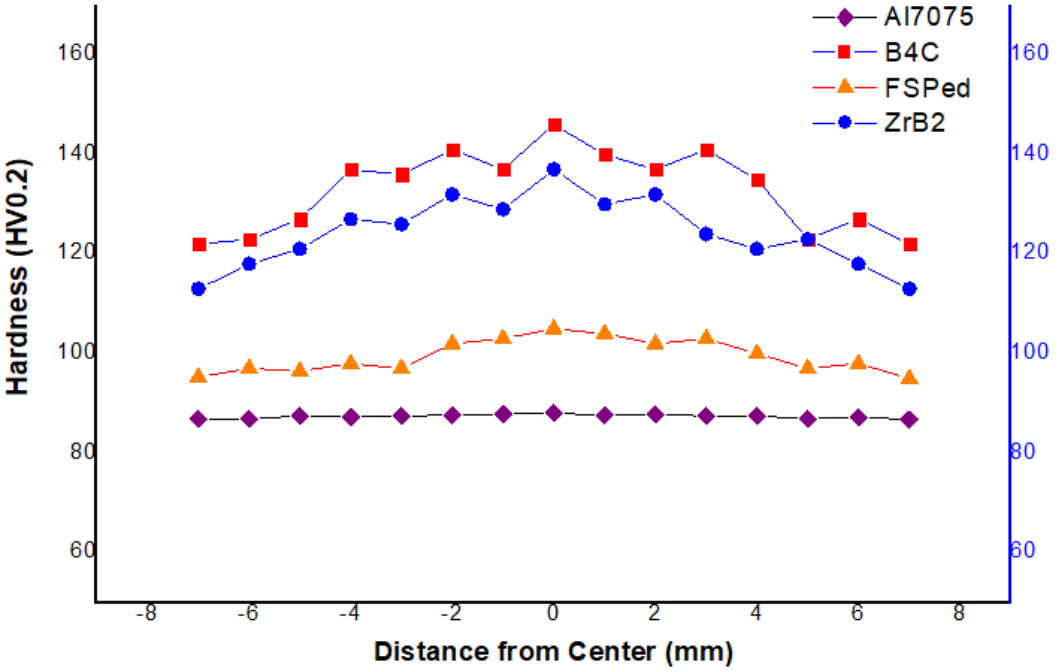

FIGURE 4.2: Hardness (HV) profile of the specimens

of the reinforcements can obtained the similar hardness values throughout the surface.

4.2 Tensile Testing Results

Universal Testing Machine was used to perform tensile testing on the prepared samples. Three samples from each pass, as well as the base metal, were prepared for tensile testing, as indicated in the preceding chapter. The tensile testing specimens were prepared to explore the tensile properties of the friction stir treated region. The specimens' gauge length is inside the processed width, which is equal to shoulder diameter. It was expected that the tensile strength of the treated zone would rise.

Tensile testing specimens of identical gauge length and area were generated for the comparative study approach's validation of the results. All of the samples were tensile tested at a constant strain rate of 2 mm/min. The flow curves compare the

mechanical properties of basic metal with those of composites made with ZrB2 and B4C particles added. One pass of FSP increases the tensile strength significantly. When the ZrB2 and B4C particles were added, the material's strength was improved when compared to the basic metal, but it was decreased when compared to the single-pass FSP route. It was caused by a decrease in ductility, which was visible due to the ceramics' brittleness. The tensile strength can be improved even more by using a multi-pass technique. Friction stir processing is a grain refining technique, and the particles ZrB2 and B4C are high-strengthening materials. The strength was improved by combining the two, as evidenced by hardness tests, and the loss of ductility in surface composites is attributable to the reinforcements. The UTM results demonstrate a reduction of tensile strength in composites, as well as the fracture surface indicating the brittle failure nature of tensile specimens. The maximum tensile strength of the specimens was shown below.

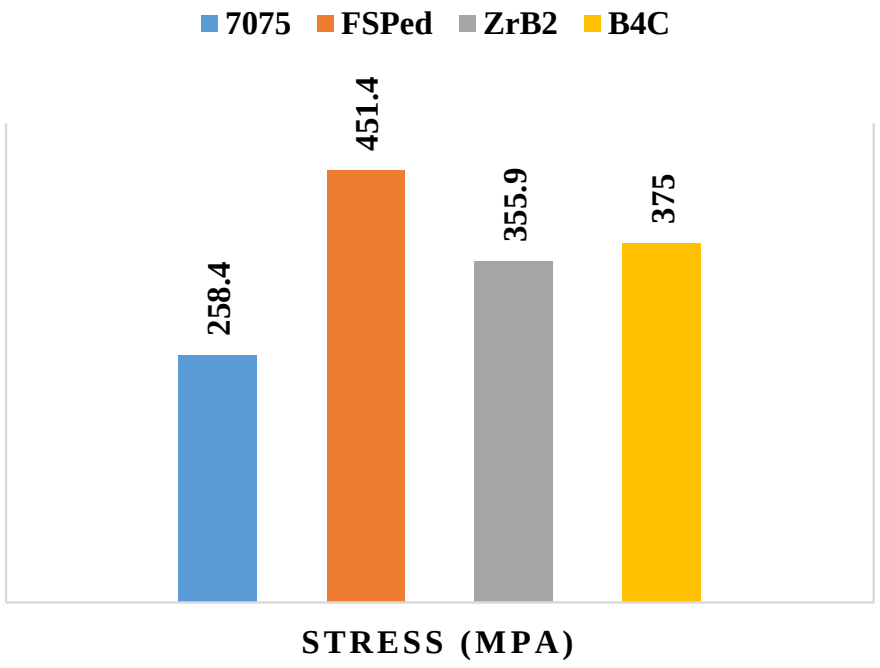

FIGURE 4.3: Comparison of the maximum tensile strength

Fig. 4.4 depicts the results of the tensile test specimens after they had been tested. Base metal (Al7075) samples exhibit necking, which can be observed. Furthermore, it can be shown from the stress-elongation curve that the material has ductile properties. A better grain structure and increased ductility are achieved

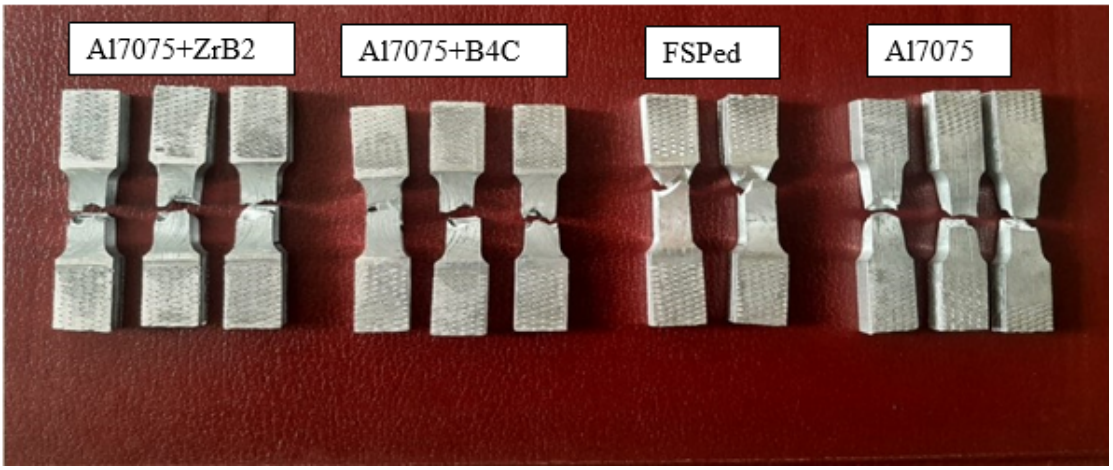

FIGURE 4.4: Tensile specimens after testing

through friction stir processing of base material without the use of reinforcement. The workability and ductility of the material are also improved.

Santella et al [32] studied the effects of friction stir processing on cast A319 and A356 and reported the increase in tensile strength and ductility of both materials in FSPed samples. The ductility of the ceramic was diminished as a result of the inclusion of ZrB2 and B4C, which was related to the brittle nature of the ceramic's enforcement. The homogeneous distribution of the particles increased the tensile strength of the composites, and the loss in percentage elongation was attributed to the reduced ductility of the material as a result of the presence of ceramics, which are hard and brittle in nature [30]. As shown in Fig. 4.4, the samples of Al7075+B4C and Al7075+ZrB2 have been subjected to testing, which has revealed that fracture happens the same way as it does in brittle materials.

Below are stress-elongation curves for base metal, processed plate without reinforcement, and composites made with B4C and ZrB2. Tensile properties of friction stir treated samples are superior to those of base metal and reinforcement samples. Because of the grain refinement of the base material Al7075, the maximum strength of the FSPed surface without reinforcement is higher. Surface composites with lower elongation indicate reduced ductility due to the presence of B4C and ZrB2. The tensile strength of the composites can also be improved by the increase in number of passes.

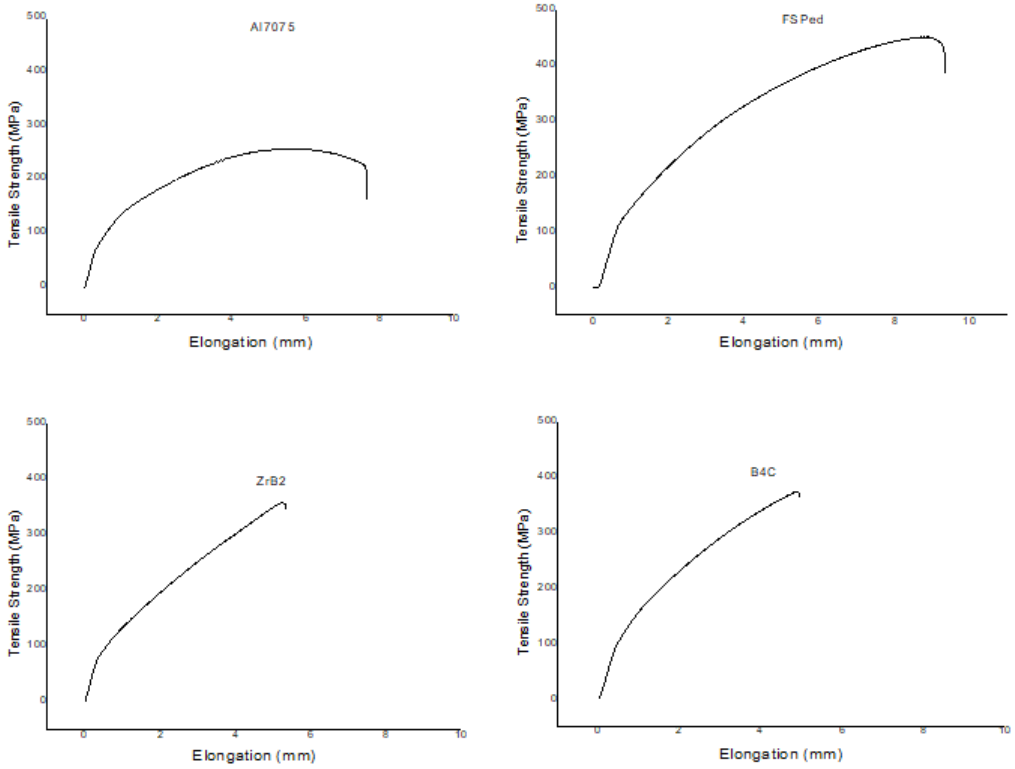

FIGURE 4.5: Tensile strength and Elongation trend of the specimens

FSPed specimens had higher strength when compared to specimen composites made with B4C and ZrB2, which may be due to better grain refining experienced by the FSPed sample. There was a significant reduction in percentage elongation of the composites in comparison to Al7075 and FSPed. This could be due to the presence of reinforcement particles, which prevented disarticulation from occurring during FSP and thus prevented the crack from propagating for an extended period of time, resulting in lower percentage elongation.

4.3 Wear Testing Results

Surface composites are manufactured to get higher values of hardness and wear resistance as compared to the base metal (Al7075). So, keeping in view wear testing was performed on a pin on disc MT/10. . . ..60/ MICRO TEST Tribometer system. A set of weights are available to provide the normal force up to 60 N, Base metal and FSPed samples (with and without enforcements) were subjected

to a normal force of 30 N and the sliding distance of 200 m. All the tests were performed using a pin of 6 mm diameter and at 200 rpm. The results of the coefficient of friction are shown below in the figure. It can be seen that the COF of the base metal (Al7075) has a higher value, following by a without enforcement FSP pass and then with ZrB2 and B4C surface composites respectively.

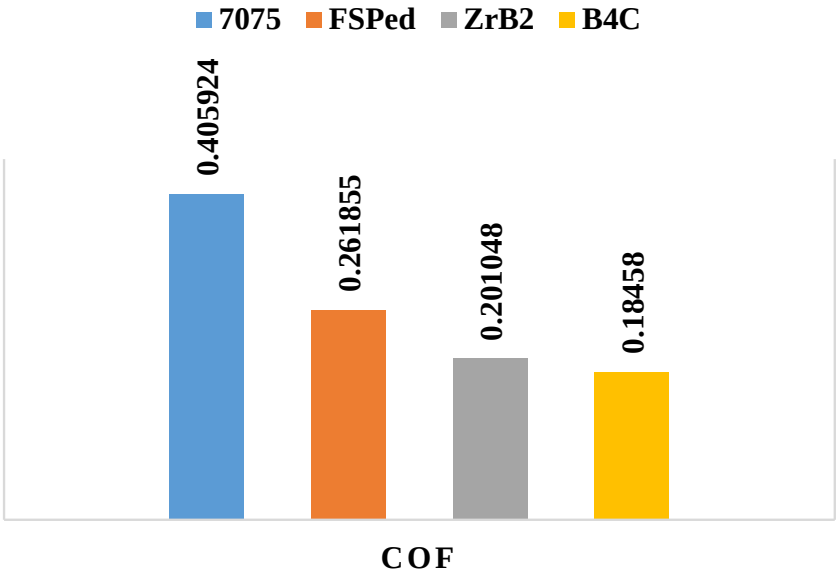

FIGURE 4.6: Average Co-efficient of Friction values

The above bar chart shows that the average coefficient of friction (COF) value for Al7075 is 0.405924, whereas the average values for FSPed, ZrB2, and B4C passes are 0.261855, 0.201048, and 0.18458, respectively. The coefficient of friction decreases as the material's hardness increases. The average value of COF indicates that the hardness of the base metal is lower than that of the FSPed sample, whereas the hardness of composite materials is higher than that of the FSPed sample. In the graph below, the COF values for base metal, FSPed sample, with ZrB2 and B4C were shown across the sliding distance. It has also been demonstrated in previous studies that surface composites manufactured by friction stir processing method must have a lower coefficient of friction value[24][37]. When the value of COF is compared to the FSPed sample with and without reinforcement, it is clear that the wear rate of base metal is higher and the wear resistance is lower than with the FSPed sample. It was clearly stated that there is an inverse relationship

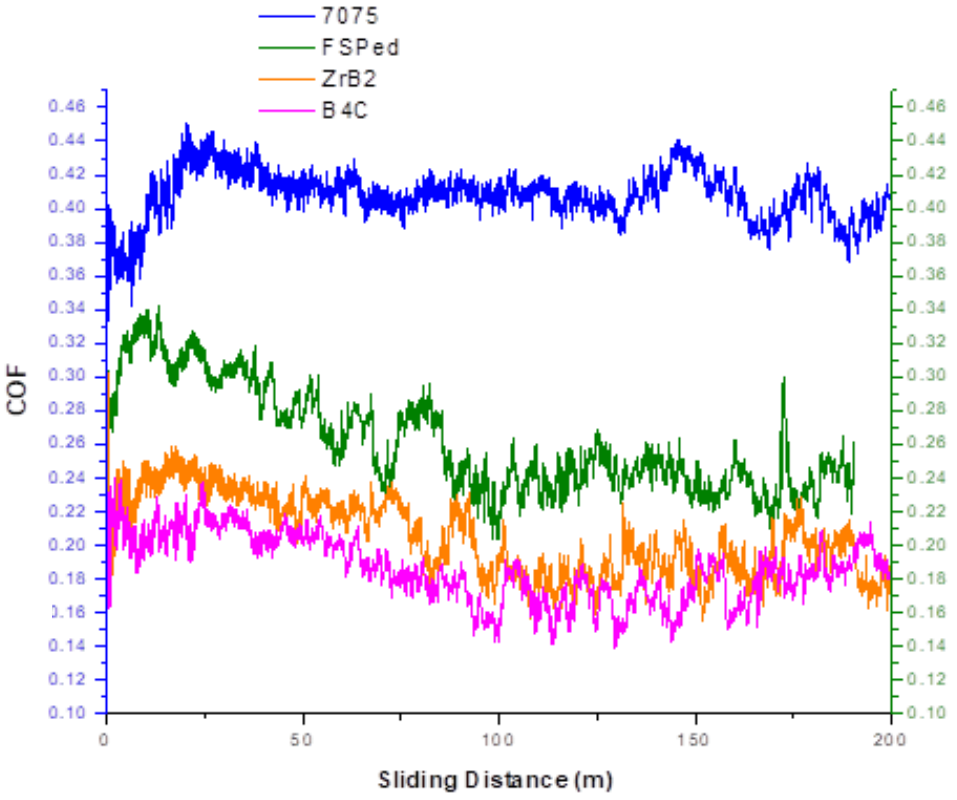

FIGURE 4.7: Comparison of COF of surface composites with FSPed and BM

between the coefficient of friction of the samples and their hardness[36]. The result of coefficient of friction values of base metal (Al7075) and the surface composite (Al7075+B4C) has similar values as presented by Karpasand et al. [8]. They have studied the effect of TiB2 and B4C particles on the tribological behavior. As the Al7075+ ZrB2 surface composite manufactured by friction stir processing was not done before but the results achieved were near to the results of Al7075+B4C surface composite. Al7075+ZrB2 have higher value of COF than Al7075+B4C, it means that the B4C surface composite have less wear rate and higher surface resistance. It was concluded that the surface composites have better wear resistance than the friction stir processed sample and base material (Al7075). The values of coefficient of friction of all the samples were plotted over the sliding distance of 200m in Fig. 4.7.

The weight of the samples was verified on a digital weighing balance before and

TABLE 4.1: Weight loss in specimens as a result of the wear test

Samples	**Weight before (grams)**	**Weight after (grams)**	**Weight loss (grams)**
7075	4.451	4.447	0.004
FSPed	4.465	4.462	0.003
ZrB2	4.182	4.18	0.002
B4C	4.429	4.427	0.002

after the wear test in order to calculate the weight loss that occurred throughout the testing. The computation of weight loss was carried out in order to validate the results of the wear tests. To determine the wear resistance of the material, simple physical phenomena were used to test it. When comparing the highest weight difference before and after the wear test, the maximum weight difference shows that the material has poorer wear resistance than when comparing the minimum weight difference. The findings of the weight reduction in specimens are shown in Table 4.1. As can be observed in the table, the base metal sample has the greatest weight loss/difference (0.004 grammes), followed by the FSPed sample, and finally the ZrB2 and B4C samples. The results show that the manufactured composite has better wear resistance than both the FSPed sample and the base metal, which is a positive finding. This is because the weighing balance had the least count of 0.001 gram, resulting in the identical weight loss for the B4C and ZrB2 samples; however, a higher accuracy weighing machine could reveal a difference in the values.

4.4 Metallography

The metallographic samples were prepared according to standard metallographic procedures. To complete the grinding and polishing of the samples, a range of sandpaper grades were used, and Keller's reagent composition was used to etch the samples before they were inspected under an optical microscope. M1, M2, M3, and M4 specimens were photographed using an optical microscope at the same magnification, demonstrating the differences in the views. The particles in sample M1 are scattered over the surface, whereas the particles in samples M2,

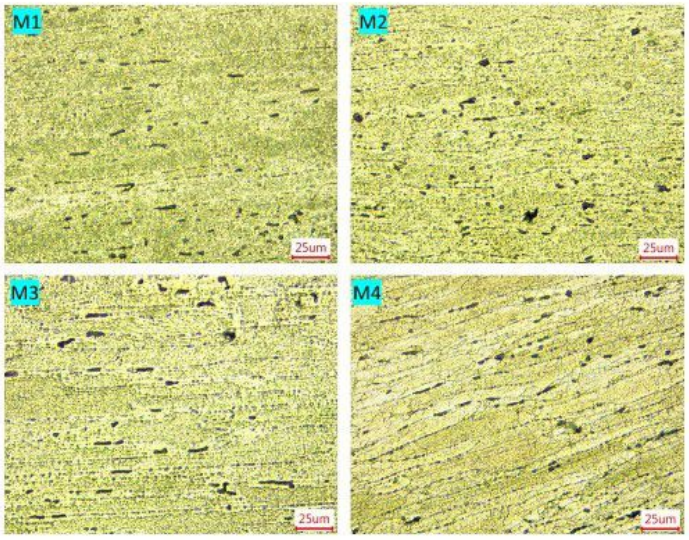

FIGURE 4.8: Metallographically results of M1, M2, M3 & M4 specimen

M3, and M4 were oriented in the direction of tool motion. That is to say, the rotation of the tool caused a change in microstructure. In M3 and M4 samples, ZrB2 and B4C particles may also be seen.

Fig. 4.8 depicts the microscopic results.

4.5 Scanning Electron Microscopy

The dispersion of B4C and ZrB2 particles in the FSPed surface composites was investigated using scanning electron microscopy (SEM). Initial preparation of SEM samples included grinding and polishing the samples, followed by suitable etching with Keller's aluminum-etching solution, as shown in the table. 3.6.

The size and shape of B4C and ZrB2 particles have been investigated using scanning electron microscopy (SEM). EDS analysis has been performed on these particles, and an approximate quantitative analysis of the particles reveals the composition of the spectrum selected as well as the presence of B4C and ZrB2 particles in the M3 and M4 samples. The results of the EDS analysis show that the particles are composed of B4C and ZrB2 atoms.

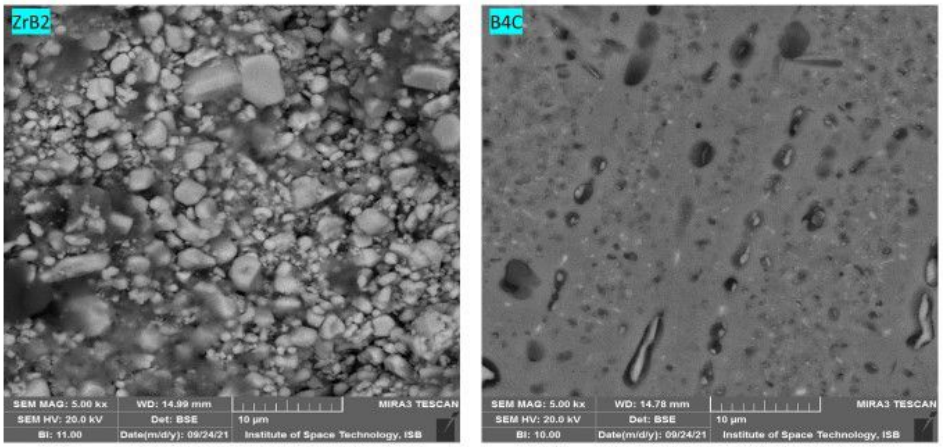

FIGURE 4.9: Results of SEM (ZrB2 & B4C composites)

4.6 Energy-Dispersive X-ray Spectrum (EDS)

Figure 4.10 shows the energy-dispersive X-ray spectrum of the surface composite Al7075+ZrB2 along with associated mapping pictures. The EDS pictures reveal a larger interfacial reaction zone, with significant levels of Al, Mg, Zn, oxygen, and carbon present. Furthermore, as reinforcements are applied, Zr and B appear in the final product. Figure depicts the presence of elements in the specified spectrum, together with their weight and atomic proportion. It depicts the phase distribution and verifies the elemental presence in the surface composite that has been created. Because two different types of particles are shown in SEM, two pictures were chosen for EDS mapping. The amount of aluminum matrix material and ZrB2 content present in the phase as seen in the images. It's because the frictional heat plastically distorted the aluminum matrix material below its melting temperature during the FSP, causing the matrix to soften. The ceramic particle ZrB2, on the other hand, has a high hardness and melting temperature, making it harder to diffuse at lower FSP temperatures. Other elements, like as carbon and oxygen, can be visible due to chemical and metallurgical reactions that occur throughout the FSP.

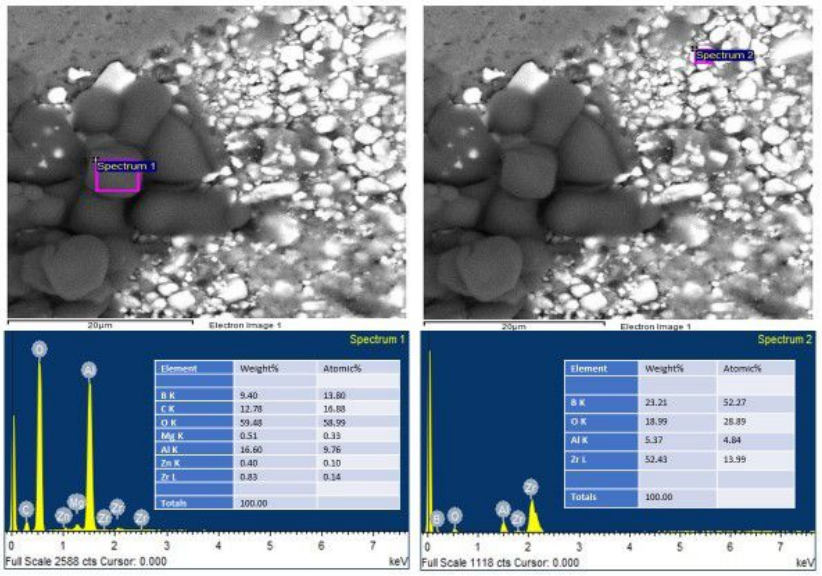

FIGURE 4.10: EDS result of Al7075+ZrB2

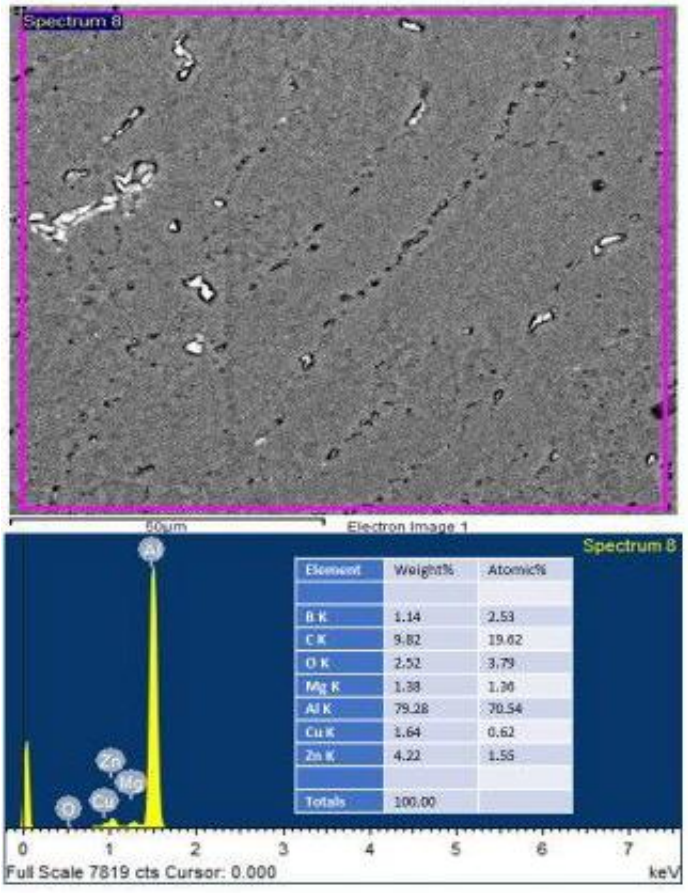

FIGURE 4.11: EDS result of Al7075+B4C composite

Figure 4.11 is the energy-dispersive X-ray spectrum of the surface composites Al7075+B4C along with the supporting mapping pictures. As the EDS picture show that the maximum area of the image was selected for the composition of the specimen with significant level of Mg, Al, Zn, Cu, oxygen and carbon. As the reinforcement the Boron and carbon was also appeared in final spectrum that shows the presence of boron carbide in the specimen. The SEM images of the Al7075+B4C has not shown any visible particles of the reinforcement which might be due to the distribution of the particles or might be due to the unavailability of the particles on the cross-section selected for the SEM. But the EDS spectrum of the image shows boron content in the composition that ensures that the particles of boron carbide were well distributed throughout the surface.

Chapter 5

Conclusion and Future Recommendations

5.1 Conclusions

The study's objective was to fabricate the surface composite and compare its mechanical properties to the base metals. The aim is to strengthen the microstructure by adding reinforcement, which would result in a significant improvement following FSP. The emphasis was on the material's hardness, Tensile strength and wear resistance, which also demonstrates positive variation. Thus, the surface composites are hardened, then the FSPed surface and FSPed surface are hardened, then the base metal.

- In this research work, surface composites were prepared and utilized for evaluating the mechanical and micro-structural properties under friction stir processing methods. The strength of Al-7075 was improved by adding ZrB2 and B4C reinforcement materials.
- Mechanical testing was carried out on different machine to investigate tribological behavior, tensile strength, hardness and microstructural trends of base metal (Al-7075), FSPed surfaces (with and without reinforcement). It

was quantitatively found that addition of reinforcement material in base metal can significantly enhance the mechanical properties of base metals as compared to without reinforcement material.

- Surface hardness of the specimens were increased by a factor of 1.20, 1.58 and 1.68 when compared to Al7075 (HV86.62) and the decreasing order was (Al-7075+ B4C, Al-7075+ ZrB2, Al-7075+FSPed and Al-7075).

- Wear testing was also carried out to investigate the wear properties of the base metal, FSPed sample and ZrB2 and B4C samples.

- Coefficient of friction was reduced in processed samples that indicates the higher wear resistance. Average COF of the FSPed, ZrB2 and B4C was decreased by 0.645, 0495, and 0.454 as compared to average value of Al7075 (0.405924).

- Tensile strength of the FSPed sample has maximum value of 451 MPa. Tensile strength of B4C and ZrB2 samples was also improved by a factor of 1.45 and 1.38 to base material.

5.2 Future Recommendations

- The researchers did not utilize zirconium diboride extensively for surface composition, and the results produced by ZrB2 were similar to B4C. Several Aluminum Matrix Composites would be created by combining ZrB2 with various base materials.

- To achieve better mechanical characteristics, Al7075+ZrB2 surface composites may be produced using a variety of reinforcing strategies.

- The use of multi-pass friction stir processing to improve the tensile strength of Al7075/ZrB2 surface composite may be explored.

- By changing the weight percentage of both reinforcements, a hybrid composite of ZrB2 and B4C may also be produced.

- Several combinations of FSP process parameters can applied for the comparison of the results.
- Study can be carried out on the corrosion and fracture resistance of ZrB2 and B4C surface composites.

REFERENCES

[1] A. R. Patel, D. J. Kotadiya, J. M. Kapopara, C. G. Dalwadi, N. P. Patel, and H. G. Rana, "Investigation of Mechanical Properties for Hybrid Joint of Aluminium to Polymer using Friction Stir Welding (FSW)," Mater. Today Proc., vol. 5, no. 2, pp. 4242–4249, 2018, doi: 10.1016/j.matpr.2017.11.688.

[2] S. Azeez and E. Akinlabi, "Sustainability of manufacturing technology: friction stir welding in focus," Prog. Ind. Ecol., vol. 12, no. 4, pp. 419–438, 2018, doi: 10.1504/PIE.2018.097188.

[3] L. Zhou et al., "New technique of self-refilling friction stir welding to repair keyhole," vol. 17, no. 8, pp. 649–655, 2012, doi: 10.1179/1362171812Y.0000000058.

[4] T. Watanabe, H. Takayama, and A. Yanagisawa, "Joining of aluminum alloy to steel by friction stir welding," J. Mater. Process. Technol., vol. 178, no. 1–3, pp. 342–349, 2006, doi: 10.1016/j.jmatprotec.2006.04.117.

[5] M. S. Dahiya, V. Kumar, and S. Verma, "A critical review on friction stir welding of dissimilar aluminium alloys," Lect. Notes Mech. Eng., pp. 707–719, 2019, doi: 10.1007/978-981-13-6412-9-66.

[6] D. K. Sharma, V. Patel, V. Badheka, K. Mehta, and G. Upadhyay, "Fabrication of Hybrid Surface Composites AA6061/(B4C + MoS2) via Friction Stir Processing," J. Tribol., vol. 141, no. 5, 2019, doi: 10.1115/1.4043067.

[7] N. Pol, G. Verma, R. P. Pandey, and T. Shanmugasundaram, "Fabrication of AA7005/TiB2-B4C surface composite by friction stir processing: Evaluation

of ballistic behaviour," Def. Technol., vol. 15, no. 3, pp. 363–368, 2019, doi: 10.1016/j.dt.2018.08.002.

[8] F. Karpasand, A. Abbasi, and M. Ardestani, "Effect of amount of TiB2 and B4C particles on tribological behavior of Al7075/B4C/TiB2 mono and hybrid surface composites produced by friction stir processing," Surf. Coatings Technol., vol. 390, no. December 2019, p. 125680, 2020, doi: 10.1016/j.surfcoat.2020.125680.

[9] R. K. Tiwari, A. Bharti, H. Tripathi, N. Kumar, and K. K. Saxena, "A re-investigation of mechanical properties of aluminium-based surface composites prepared by friction stir processing," Mater. Today Proc., vol. 45, no. xxxx, pp. 4550–4557, 2021, doi: 10.1016/j.matpr.2020.12.1220.

[10] R. Ande, P. Gulati, D. K. Shukla, and H. Dhingra, "ScienceDirect Microstructural and Wear Characteristics of Friction Stir Processed Al-7075 / SiC Reinforced Aluminium Composite," Mater. Today Proc., vol. 18, pp. 4092–4101, 2019, doi: 10.1016/j.matpr.2019.07.353.

[11] K. A. Prabha, P. K. Putha, and B. S. Prasad, "Effect of tool rotational speed on mechanical properties of aluminium alloy 5083 weldments in friction stir welding," Mater. Today Proc., vol. 5, no. 9, pp. 18535–18543, 2018, doi: 10.1016/j.matpr.2018.06.196.

[12] J. Jamal, B. Darras, and H. Kishawy, "A study on sustainability assessment of welding processes," Proc. Inst. Mech. Eng. Part B J. Eng. Manuf., vol. 234, no. 3, pp. 501–512, 2020, doi: 10.1177/0954405419875355.

[13] P. L. Threadgill, "Terminology in friction stir welding," Sci. Technol. Weld. Join., vol. 12, no. 4, pp. 357–360, 2007, doi: 10.1179/174329307X197629.

[14] M. S. Sidhu and S. S. Chatha, "Friction Stir Welding Process and its variables : A Review," Int. J. Emerg. Technol. Adv. Eng., vol. 2, no. 12, pp. 275–279, 2012.

[15] M. Akbari, R. Abdi Behnagh, and A. Dadvand, "Effect of materials position on friction stir lap welding of Al to Cu," Sci. Technol. Weld. Join., vol. 17, no. 7, pp. 581–588, 2012, doi: 10.1179/1362171812Y.0000000049.

[16] T. Saeid, A. Heidarzadeh, K. Darzi, and M. Ashjari, "Effect of tool pin profile on microstructure and mechanical properties of friction stir welded AZ31B magnesium alloy," J. Mater., 2014, doi: 10.1016/j.matdes.2014.02.068.

[17] R. S. Mishra and Z. Y. Ma, "Friction stir welding and processing," Mater. Sci. Eng. R Reports, vol. 50, no. 1–2, pp. 1–78, 2005, doi: 10.1016/j.mser.2005.07.001.

[18] A. Shrivastava, M. Krones, and F. E. Pfefferkorn, "Comparison of energy consumption and environmental impact of friction stir welding and gas metal arc welding for aluminum," CIRP J. Manuf. Sci. Technol., vol. 9, pp. 159–168, 2015, doi: 10.1016/j.cirpj.2014.10.001.

[19] Y. S. Sato and H. Kokawa, "Friction stir welding (FSW) process," Weld. Int., vol. 17, no. 11, pp. 852–855, 2003, doi: 10.1533/wint.2003.3174.

[20] L. I. U. H. Ye and Z. Hui-jie, "Repair welding process of friction stir welding groove defect," Trans. Nonferrous Met. Soc. China, vol. 19, no. 3, pp. 563–567, 2008, doi: 10.1016/S1003-6326(08)60313-1.

[21] G. Buffa, D. Campanella, R. Di Lorenzo, L. Fratini, and G. Ingarao, "Analysis of Electrical Energy Demands in Friction Stir Welding of Aluminum Alloys," Procedia Eng., vol. 183, pp. 206–212, 2017, doi: 10.1016/j.proeng.2017.04.022.

[22] Z. Y. Ma, "Friction stir processing technology: A review," Metall. Mater. Trans. A Phys. Metall. Mater. Sci., vol. 39 A, no. 3, pp. 642–658, 2008, doi: 10.1007/s11661-007-9459-0.

[23] G. Huang, W. Hou, J. Li, and Y. Shen, "Development of surface composite based on Al-Cu system by friction stir processing: Evaluation of microstructure, formation mechanism and wear behavior," Surf. Coatings Technol., vol. 344, no. October 2017, pp. 30–42, 2018, doi: 10.1016/j.surfcoat.2018.03.005.

[24] H. Rana and V. Badheka, "Influence of friction stir processing conditions on the manufacturing of Al-Mg-Zn-Cu alloy/boron carbide surface composite," J. Mater. Process. Technol., vol. 255, pp. 795–807, 2018, doi: 10.1016/j.jmatprotec.2018.01.020.

[25] K. P. Mehta, "Sustainability in Welding and Processing," pp. 125–145, 2019, doi: 10.1007/978-3-030-03276-0-6.

[26] H. Kumar, R. Prasad, A. Srivastava, M. Vashista, and M. Z. Khan, "Utilisation of industrial waste (Fly ash) in synthesis of copper based surface composite through friction stir processing route for wear applications," J. Clean. Prod., vol. 196, pp. 460–468, 2018.

[27] S. Rathee, S. Maheshwari, A. N. Siddiquee, and M. Srivastava, "Distribution of reinforcement particles in surface composite fabrication via friction stir processing: Suitable strategy," Mater. Manuf. Process., vol. 33, no. 3, pp. 262–269, 2018, doi: 10.1080/10426914.2017.1303147.

[28] M. S. Weglowski, "Friction stir processing – State of the art," Arch. Civ. Mech. Eng., vol. 18, no. 1, pp. 114–129, 2018, doi: 10.1016/j.acme.2017.06.002.

[29] V. K. S. Jain, J. Varghese, and S. Muthukumaran, "Effect of First and Second Passes on Microstructure and Wear Properties of Titanium Dioxide-Reinforced Aluminum Surface Composite via Friction Stir Processing," Arab. J. Sci. Eng., vol. 44, no. 2, pp. 949–957, 2019, doi: 10.1007/s13369-018-3312-1.

[30] H. Kumar, R. Prasad, and P. Kumar, "Effect of multi-groove reinforcement strategy on Cu/SiC surface composite fabricated by friction stir processing," Mater. Chem. Phys., vol. 256, no. May, p. 123720, 2020, doi: 10.1016/j.matchemphys.2020.123720.

[31] M. Barati, M. Abbasi, and M. Abedini, "The effects of friction stir processing and friction stir vibration processing on mechanical, wear and corrosion characteristics of Al6061/SiO2 surface composite," J. Manuf. Process., vol. 45, no. March, pp. 491–497, 2019, doi: 10.1016/j.jmapro.2019.07.034.

[32] M. L. Santella, T. Engstrom, D. Storjohann, and T. Y. Pan, "Effects of friction stir processing on mechanical properties of the cast aluminum alloys A319 and A356," Scr. Mater., vol. 53, no. 2, pp. 201–206, 2005, doi: 10.1016/j.scriptamat.2005.03.040.

[33] M. A. García-Bernal, R. S. Mishra, R. Verma, and D. Hernández-Silva, "Hot deformation behavior of friction-stir processed strip-cast 5083 aluminum alloys with different Mn contents," Mater. Sci. Eng. A, vol. 534, pp. 186–192, 2012, doi: 10.1016/j.msea.2011.11.057.

[34] S. K. Patel, V. P. Singh, B. S. Roy, and B. Kuriachen, "Recent research progresses in Al-7075 based in-situ surface composite fabrication through friction stir processing: A review," Mater. Sci. Eng. B Solid-State Mater. Adv. Technol., vol. 262, no. September, p. 114708, 2020, doi: 10.1016/j.mseb.2020.114708.

[35] F. García-vázquez, B. Vargas-arista, R. Muñiz, J. C. Ortiz, and H. H. García, "The Role of Friction Stir Processing (FSP) Parameters on TiC Reinforced Surface Al7075-T651 Aluminum Alloy," vol. 21, no. 4, pp. 508–516, 2017.

[36] S. Bharti, N. D. Ghetiya, and V. Dutta, "Investigating microhardness and wear behavior of Al5052/ZrO2surface composite produced by friction stir processing," Mater. Today Proc., vol. 44, no. xxxx, pp. 52–57, 2021, doi: 10.1016/j.matpr.2020.06.318.

[37] K. Periasamy, N. Sivashankar, S. Chandrakumar, and R. Viswanathan, "Measurement of Friction and Wear in Aluminum Alloy Al7075 / Sic & Gr Processed By Friction Stir Method," no. February, 2020, doi: 10.35940/ijitee.C8480.019320.

[38] K. Elangovan and V. Balasubramanian, "Influences of tool pin profile and welding speed on the formation of friction stir processing zone in AA2219 aluminium alloy," J. Mater. Process. Technol., vol. 200, no. 1–3, pp. 163–175, 2008, doi: 10.1016/j.jmatprotec.2007.09.019.

[39] S. Rathee, S. Maheshwari, A. N. Siddiquee, and M. Srivastava, "Effect of tool plunge depth on reinforcement particles distribution in surface composite fabrication via friction stir processing," Def. Technol., vol. 13, no. 2, pp. 86–91, 2017, doi: 10.1016/j.dt.2016.11.003.

[40] A. K. Srivastava, N. K. Maurya, A. R. Dixit, S. P. Dwivedi, A. Saxena, and M. Maurya, "Experimental investigations of A359/Si3N4 surface composite produced by multi-pass friction stir processing," Mater. Chem. Phys., vol. 257, no. September 2020, p. 123717, 2021, doi: 10.1016/j.matchemphys.2020.123717.

[41] N. Gangil, S. Maheshwari, and A. N. Siddiquee, "Multipass FSP on AA6063-T6 Al: Strategy to fabricate surface composites," Mater. Manuf. Process., vol. 33, no. 7, pp. 805–811, 2018, doi: 10.1080/10426914.2017.1415448.

[42] S. P. M, E. P. A, and A. S, "Development of multi-pass processed AA6082/SiCp surface composite using friction stir processing and its mechanical and tribology characterization," Surf. Coatings Technol., vol. 394, no. December 2019, p. 125900, 2020, doi: 10.1016/j.surfcoat.2020.125900.

[43] M. K. Gupta, "Friction Stir Process : A Green fabrication technique - A Review Paper, " SN Appl. Sci., vol. 2, no. 4, pp. 1–14, 2020, doi: 10.1007/s42452-020-2330-2.

[44] H. G. Rana, V. J. Badheka, and A. Kumar, "Fabrication of Al7075 / B4C Surface Composite by Novel Friction Stir Processing (FSP) and Investigation on Wear Properties," Procedia Technol., vol. 23, pp. 519–528, 2016, doi: 10.1016/j.protcy.2016.03.058.

[45] S. Bharti, N. D. Ghetiya, and K. M. Patel, "A review on manufacturing the surface composites by friction stir processing," Materials

and Manufacturing Processes, vol. 36, no. 2. pp. 135–170, 2021, doi: 10.1080/10426914.2020.1813897.

[46] S. M, S. Rao.CH, and M. Saheb.K, "ScienceDirect PMME 2016 Production of Surface Composites by Friction Stir Processing," Mater. Today Proc., vol. 5, no. 1, pp. 929–935, 2018, doi: 10.1016/j.matpr.2017.11.167.

[47] D. S. C. Mouli and R. U. Rao, "Optimization of Friction Stir Process Parameters for Micro- Hardness and Wear Characteristics of Silicon Carbide-Reinforced Al-7075 Surface Composite," Trans. Indian Inst. Met., 2021, doi: 10.1007/s12666-021-02394-4.

[48] N. Dialami, M. Cervera, and M. Chiumenti, "Effect of the tool tilt angle on the heat generation and the material flow in friction stir welding," Metals (Basel)., vol. 9, no. 1, 2019, doi: 10.3390/met9010028.

[49] K. R. Seighalani, M. K. B. Givi, A. M. Nasiri, and P. Bahemmat, "Investigations on the Effects of the Tool Material , Geometry , and Tilt Angle on Friction Stir Welding of Pure Titanium," vol. 19, no. October, pp. 955–962, 2010, doi: 10.1007/s11665-009-9582-8.

[50] N. A. Patil, A. Safwan, S. R. Pedapati, and R. H. Ash, "Materials Today : Proceedings Effect of Deposition Methods on micro structure and mechanical properties of AA 7075 Alloy - rice husk ash surface composites using friction stir processing, " Mater. Today Proc., no. November 2018, 2020, doi: 10.1016/j.matpr.2020.05.639.

[51] K. Kumar and S. V. Kailas, "The role of friction stir welding tool on material flow and weld formation," Mater. Sci. Eng. A, vol. 485, no. 1–2, pp. 367–374, 2008, doi: 10.1016/j.msea.2007.08.013.

[52] M. K. Sued, S. S. M. Samsuri, M. K. A. M. Kassim, and S. N. N. M. Nasir, "Sustainability of Welding Process through Bobbin Friction Stir Welding," IOP Conf. Ser. Mater. Sci. Eng., vol. 318, no. 1, 2018, doi: 10.1088/1757-899X/318/1/012068.

[53] R. Butola, M. S. Ranganath, and Q. Murtaza, "Fabrication and optimization of AA7075 matrix surface composites using Taguchi technique via friction stir processing (FSP)," Eng. Res. Express, vol. 1, no. 2, 2019, doi: 10.1088/2631-8695/ab4b00.

[54] G. Ghangas and S. Singhal, "ScienceDirect Investigations of Multi-pass Friction Stir Welding for Al-Zn-Mg Alloy," vol. 5, pp. 17107–17113, 2018, doi: 10.1016/j.matpr.2018.04.118.

[55] R. Butola, Q. Murtaza, and R. M. Singari, "Formation of Self-Assembled Monolayer and Characterization of AA7075-T6/B4C Nano-ceramic surface composite using Friction Stir Processing," Surf. Topogr. Metrol. Prop., 2020, [Online]. Available: https://iopscience.iop.org/article/10.1088/2053-1583/abe778.

[56] R. Ande, P. Gulati, D. K. Shukla, and H. Dhingra, "Microstructural and wear characteristics of friction stir processed Al-7075/SiC reinforced aluminium composite," Mater. Today Proc., vol. 18, pp. 4092–4101, 2019, doi: 10.1016/j.matpr.2019.07.353.

[57] S. Rathee, S. Maheshwari, A. N. Siddiquee, and M. Srivastava, "A Review of Recent Progress in Solid State Fabrication of Composites and Functionally Graded Systems Via Friction Stir Processing," Crit. Rev. Solid State Mater. Sci., vol. 43, no. 4, pp. 334–366, 2018, doi: 10.1080/10408436.2017.1358146.

[58] S. R. Strand, C. D. Sorensen, and T. W. Nelson, "Effects of friction stir welding on polymer microstructure," Annu. Tech. Conf. - ANTEC, Conf. Proc., vol. 1, pp. 1078–1082, 2003.

[59] T. Thankachan, K. S. Prakash, and V. Kavimani, "Investigations on the effect of friction stir processing on Cu-BN surface composites," Mater. Manuf. Process., vol. 33, no. 3, pp. 299–307, 2018, doi: 10.1080/10426914.2017.1291952.

[60] D. Yadav and R. Bauri, "Effect of friction stir processing on microstructure and mechanical properties of aluminium," Mater. Sci. Eng. A, vol. 539, pp. 85–92, 2012, doi: 10.1016/j.msea.2012.01.055.

[61] J. Gao, S. Zhang, H. Jin, and Y. Shen, "Fabrication of Al7075 / PI composites base on FSW technology," pp. 4377–4386, 2019.

[62] S. Bharti, V. Dutta, S. Sharma, and R. Kumar, "A study on the effect of Friction Stir Processing on the hardness of Aluminum 6000 series," Mater. Today Proc., vol. 18, pp. 5185–5188, 2019, doi: 10.1016/j.matpr.2019.07.517.

[63] N. Saini, C. Pandey, S. Thapliyal, and D. K. Dwivedi, "Mechanical Properties and Wear Behavior of Zn and MoS2 Reinforced Surface Composite Al- Si Alloys Using Friction Stir Processing," Silicon, vol. 10, no. 5, pp. 1979–1990, 2018, doi: 10.1007/s12633-017-9710-2.

[64] S. Kumar, A. Kumar, and C. Vanitha, "ScienceDirect Corrosion behaviour of Al 7075 / TiC composites processed through friction stir processing," Mater. Today Proc., vol. 15, pp. 21–29, 2019, doi: 10.1016/j.matpr.2019.05.019.

[65] A. Kumar, K. Pal, and S. Mula, "Simultaneous improvement of mechanical strength , ductility and corrosion resistance of stir cast Al7075-2 % SiC micro- and nanocomposites by friction stir processing," J. Manuf. Process., vol. 30, pp. 1–13, 2017, doi: 10.1016/j.jmapro.2017.09.005.

[66] G. Hussain, R. Hashemi, H. Hashemi, and K. A. Al-ghamdi, "An experimental study on multi-pass friction stir processing of Al TiN composite: some microstructural , mechanical , and wear characteristics," Int. J. Adv. Manuf. Technol., pp. 533–546, 2016, doi: 10.1007/s00170-015-7504-5.

[67] A. Kumar, K. Pal, and S. Mula, "Effects of cryo-FSP on metallurgical and mechanical properties of stir cast Al7075 e SiC nanocomposites," J. Alloys Compd., vol. 852, p. 156925, 2021, doi: 10.1016/j.jallcom.2020.156925.

[68] O. M. Ikumapayi, E. T. Akinlabi, J. D. Majumdar, and S. A. Akinlabi, Applications of coconut shell ash / particles in modern manufacturing: a case study of friction stir processing. LTD, 2020.

[69] E. B. Moustafa, A. Melaibari, and M. Basha, "Wear and microhardness behaviors of AA7075 / SiC-BN hybrid nanocomposite surfaces fabricated

by friction stir processing," Ceram. Int., no. February, pp. 0–1, 2020, doi: 10.1016/j.ceramint.2020.03.274.

[70] N. A. Patil, S. R. Pedapati, O. Bin Mamat, and A. M. Lubis, Hidayat Syah, "Optimization of Friction Stir Process Parameters for Enhancement in Surface Properties of Al 7075-SiC/Gr Hybrid Surface Composites," coatings, 2019.

[71] F. Karpasand and M. Ardestani, "The effect of powder addition manner and volume fraction of reinforcement on tribological behavior of Al7075 / B 4 C surface composite produced by friction stir processing," 2020, doi: 10.1177/0021998320904143.